Brain Pacemaker

Peter A. Tass[1,2,3], Christian Hauptmann[1] and Oleksandr V. Popovych[1]
[1]Institute of Neuroscience and Medicine – Neuromodulation (INM-7), Jülich Research Center, Jülich, Germany
[2]Department of Neurosurgery, Stanford University, Stanford, CA, USA
[3]Department of Neuromodulation, University of Cologne, Cologne, Germany

Article Outline

Glossary

Coordinated reset stimulation Coordinated reset (CR) stimulation is an effectively desynchronizing control technique, where a population of synchronized oscillators is stimulated via several stimulation sites in such a way that spatially and timely coordinated phase reset is achieved in subpopulations assigned to each of the stimulation sites. This method is suggested for the counteraction of abnormal neuronal synchronization characteristic for several neurological diseases and amelioration of their symptoms. It has successively been verified in a number of experimental and clinical studies.

Deep brain stimulation Electrical deep brain stimulation (DBS) is the standard therapy for medically refractory movements disorders, e.g., Parkinson's disease and essential tremor. It requires a surgical treatment, where depth electrodes are chronically implanted in target areas like the thalamic ventralis intermedius nucleus or the subthalamic nucleus. For standard DBS electrical high-frequency (>100 Hz) stimulation is permanently delivered via depth electrodes. More sophisticated deep brain stimulation techniques are in the process of being established for clinical use.

Delayed feedback Delayed feedback is a method for the creation of a closed-loop forcing, where a portion of the measured output signal of a system is time delayed, linearly or non-linearly processed, and fed back into the system. This approach is often used to control the dynamic behavior of complex systems. In this article delayed feedback is used to control synchronization in ensembles of coupled oscillators, e.g., neurons.

Order parameter The order parameter is a quantity characterizing a phase transition or phase change in the transformation of a complex system from one phase (state) to another. The order parameter is convenient for characterizing the onset and extent of synchronization in larger ensembles: Perfect phase synchronization corresponds to a large value of the order parameter, whereas an incoherent (desynchronized) state is associated with a small value of the order parameter. In synergetics it has been shown that the dynamics of complex systems may be governed by only a few order parameters.

Synchronization Synchronization (from Greek *syn* = the same, common and *chronos* = time) means the adjustment of rhythms of self-sustained oscillators due to their weak interaction. The interacting oscillators can be regular (periodic) or chaotic. There are several different forms of synchronization including phase,

© Springer Science+Business Media, LLC, part of Springer Nature 2020

A. Hutt, H. Haken (eds.), *Synergetics*,
https://doi.org/10.1007/978-1-0716-0421-2_42

Originally published in
R. A. Meyers (ed.), *Encyclopedia of Complexity and Systems Science*, © Springer Science+Business Media LLC 2018
https://doi.org/10.1007/978-3-642-27737-5_42-2

complete, generalized, and lag synchronization, etc. In this article we focus on phase synchronization. In the simplest form, the oscillators, rotating with the same frequency, become phase synchronized (phase locked) to each other, if they tend to oscillate with the same repeating sequence of relative phase angles. Put otherwise, the oscillators adjust their rhythms, while their amplitude dynamics need not be correlated.

Definition of the Subject

A brain pacemaker is a medical device that is implanted into the brain with the purpose to stimulate nervous tissue with electrical signals. Brain pacemakers are used for the therapy of patients suffering, for example, from Parkinson's disease, epilepsy or mental disorders. Brain stimulation is either called deep brain stimulation (DBS) if structures deeply inside the brain are targeted or cortical stimulation (intracortical or epicortical), if the electrical contacts of the stimulator are positioned within the cortex or on its surface. Apart from direct brain stimulation, other targets may also be used, such as spinal cord (e.g., for the treatment of pain) or the vagus nerve (for the treatment of epilepsy). The electrical stimulation of the nervous system has a long history which goes back to the nineteenth century where first tests with cortical stimulation were documented (Gildenberg 2005). The first intraoperative deep brain stimulation was performed by Spiegel et al. in 1947 in a patient suffering from Huntington's chorea, and in the eighties DBS was introduced as a treatment for motor disorders (Brice and McLellan 1980; Benabid et al. 1987). DBS was approved by the Food and Drug Administration (FDA) as a treatment for essential tremor in 1997, for Parkinson's disease in 2002, and dystonia in 2003. The treatment of severe neurological and psychiatric diseases with brain pacemakers is a rapidly growing and promising field. Novel, model-based approaches, which use methods from synergetics, nonlinear dynamics, and statistical physics, to specifically restore brain function and connectivity, demonstrate how insights into the dynamics of complex systems contribute to the development of novel therapies.

Introduction

Self-organization processes are abundant in numerous fields of the natural sciences (Haken 1977, 1983). For instance, the nervous system elegantly utilizes self-organization principles for motor control purposes (Haken et al. 1985; Schöner et al. 1986; Haken 1996; Kelso 1995). A classical example of a self-organization process is synchronization of populations of interacting oscillators, which is widely observed in physics (Haken 1970, 1983; Pikovsky et al. 2001; Strogatz 2003), chemistry (Kuramoto 1984), biology (Winfree 1980), neuroscience (Steriade et al. 1990; Haken 2002), and medicine (Elble and Koller 1990; Milton and Jung 2003; Tass 1999). In the nervous system synchronization processes are important, e.g., in the context of information processing (Singer 1989) and motor control (Andres and Gerloff 1999). However, pathological, excessive synchronization strongly impairs brain function (Elble and Koller 1990; Milton and Jung 2003). In fact, pathological synchronization processes are the hallmark of several neurological diseases like Parkinson's disease (PD) or essential tremor (Alberts et al. 1969; Nini et al. 1995). For example, Parkinsonian resting tremor appears to be caused by a pacemaker-like population of neurons which fires in a synchronized and periodical manner (Alberts et al. 1969; Smirnov et al. 2008). In contrast, under healthy conditions these neurons fire in an uncorrelated, i.e. desynchronized manner (Nini et al. 1995).

Permanent deep brain stimulation (DBS) at high frequencies ($>$100 Hz) is the standard therapy for medically refractory patients suffering from Parkinson's disease and essential tremor (Benabid et al. 1991, 2002; Blond et al. 1992), see Fig. 1. High-frequency (HF) DBS has been developed empirically, mainly based on experimental results and clinical observations. The mechanism of HF DBS is still a matter of debate (Benabid et al. 2005). Clinical studies showed that

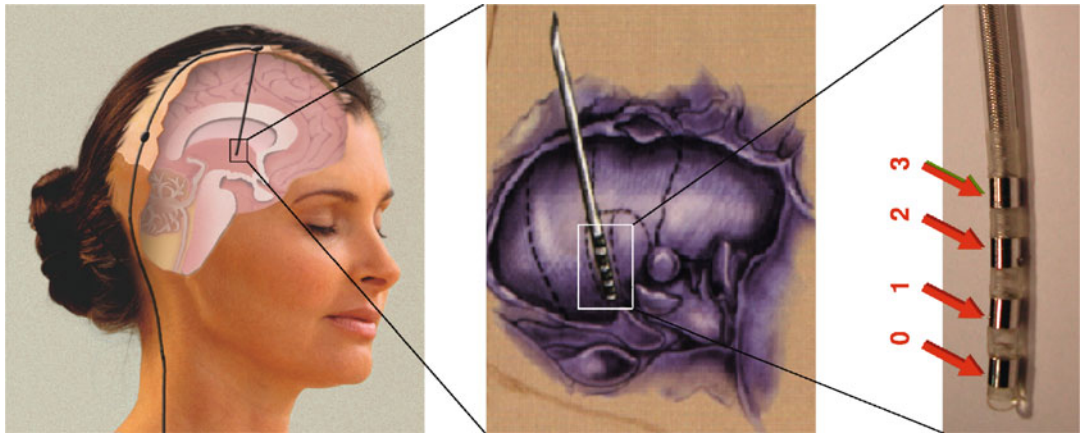

Brain Pacemaker, Fig. 1 Standard DBS setup. A depth electrode is implanted into the target structure (e.g., the *subthalamic nucleus*). The electrode is subcutaneously connected with the generator of the high-frequency stimulation signal (not shown in this image). The stimulation signal is delivered through one or more of the four stimulation contacts labeled from 0 to 3

HF DBS essentially has similar effects as observed after tissue lesioning. Compared to lesioning, DBS is reversible and has a lower rate of side effects (Tasker 1998; Schuurman et al. 2000). However, in spite of many beneficial effects, in some patients DBS may not help, or may cause side effects, or the therapeutic effects may disappear over time (Tasker 1998; Volkmann 2004; Rodriguez-Oroz et al. 2005; Deuschl et al. 2006). With the objective of finding better tolerated and more effective DBS techniques, a model-based development of novel stimulation methods has been initiated (Tass 1999, 2002a, c, 2003b; Hauptmann et al. 2005a, b, c, 2007b; Tass et al. 2006; Popovych et al. 2005, 2006a, b), see Fig. 2. In these studies, relevant neuronal target populations were modeled mathematically and stimulation techniques have been developed utilizing principles from nonlinear dynamics and statistical physics (Tass 1999).

One goal of this approach is to control the pathological neural dynamics appropriately in order to achieve a mild and efficient relief of symptoms (Tass 1999). The second, more ambitious goal is to stimulate in a way that the formerly affected neuronal populations unlearn their pathological connectivity and, hence, their tendency to produce pathological synchronization (Tass and Majtanik 2006). Put otherwise, the very goal of this approach is to induce long-lasting therapeutic effects which outlast the cessation of stimulation (Tass and Majtanik 2006; Tass and Hauptmann 2007; Hauptmann and Tass 2007). To this end, stimulation algorithms have been developed and optimized to exploit dynamic self-organization principles and plasticity rules (Tass and Majtanik 2006; Tass and Hauptmann 2006, 2007; Hauptmann and Tass 2007; Hauptmann et al. 2007b).

Several novel stimulation techniques have computationally been developed in the past. In this article four of these control methods will be presented in detail: coordinated reset (CR) stimulation (Tass 1999, 2002a, c, 2003b), multisite linear delayed feedback (MLDF) stimulation (Hauptmann et al. 2005a, b, c), nonlinear delayed feedback (NDF) stimulation (Popovych et al. 2005, 2006a, b; Popovych and Tass 2010), and proportional–integro–differential feedback (PIDF) stimulation (Pyragas et al. 2007). These techniques have the common objective of reducing the synchronized activity of the target population by reestablishing a normal desynchronized physiological activity in a highly synchronized population of neurons. For other stimulation methods we refer to Rosenblum and Pikovsky (2004a), Tukhlina et al. (2007), Kiss et al. (2007), Luo et al. (2009), Danzl et al. (2009), and Nabi and Moehlis (2011).

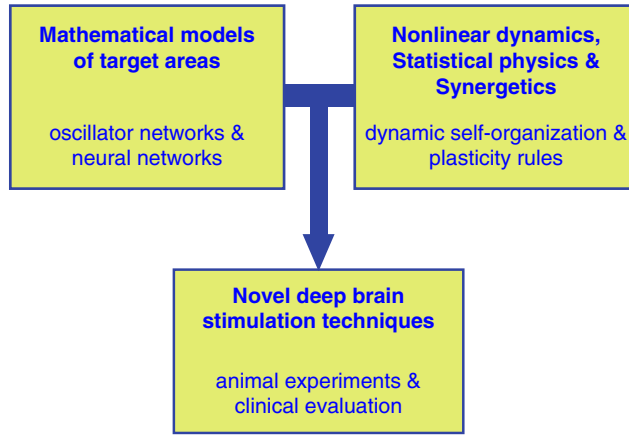

Brain Pacemaker, Fig. 2 Model-based development of novel deep brain stimulation techniques: Along the lines of a top-down approach target areas for deep brain stimulation are modeled by means of oscillator networks and physiology- and anatomy-based neural networks. Methods from nonlinear dynamics, statistical physics, and synergetics are employed to develop stimulation techniques which specifically utilize dynamic self-organization principles and plasticity rules. Experimental feedback from both animal experiments and clinical evaluation serves to validate, falsify or modify theoretical assumptions and predictions. This iterative approach aims at steadily improving the mathematically designed stimulation techniques and, hence, at establishing superior therapies

CR stimulation, in its original realization, uses short electrical pulse trains to subsequently reset sub-populations of the neuronal network, which induces a desynchronized state (Tass 1999, 2002a, c, 2003b). The stimulation is applied through a small number of stimulation sites which are equally spaced within the neuronal population. CR stimulation induced desynchronization is achieved by utilizing self-organization principles, in particular, the slaving principle induced by the pathological neuronal interactions (i.e., interactions which have the potential to induce a pathological synchronization) (Tass 2002a, c, 2003b). MLDF (Hauptmann et al. 2005a, b, c) and NDF (Popovych et al. 2005, 2006a, b; Popovych and Tass 2010) stimulation use delayed feedback for stabilizing a desynchronized state which is intended to be as close to the physiological mode of action as possible. Here, the local field potential (LFP) of the target population is measured, amplified, delayed, and fed back into the ensemble. The PIDF feedback (Pyragas et al. 2007) utilizes an instantaneous LFP and is designed for a particularly difficult situation characterized by a separate registration and stimulation setup.

It has been shown experimentally, that synaptic plasticity enhances pathological synchronization (Nowotny et al. 2003). From the kindling phenomenon in the context of epilepsy it is well known that neural networks may learn pathological strong interactions (Speckmann and Elger 1991; Morimoto et al. 2004). The novel desynchronizing stimulation protocols are designed to invert this pathological process, so that the affected neuronal populations unlearn their pathological connectivity, and physiological neuronal activity is re-established on a long-term basis. In a nutshell, the novel stimulation techniques aim at a well-directed employment of fundamental principles of dynamic brain action to induce long-lasting therapeutic effects.

Standard High-Frequency Stimulation

High-frequency (HF) deep brain stimulation (DBS) is the standard therapy for patients suffering from medically refractory PD or essential tremor (Benabid et al. 1991, 2002). To this end, depth electrodes are chronically implanted in the thalamic ventralis intermedius nucleus or the subthalamic nucleus (Benabid et al. 1991, 2002) and a permanent HF ($>$100 Hz) periodic pulse train stimulation is applied (Fig. 1). HF DBS has been

developed empirically, mainly based on intraoperative observations. HF DBS strongly alters the neuronal firing and mimics the effect of tissue lesioning, e.g., by suppressing neuronal firing, which, in turn, suppresses the peripheral tremor (Benabid et al. 2002; Filali et al. 2004; McIntyre et al. 2004b; Volkmann 2004). However, as yet, the mechanism of HF DBS is not sufficiently understood (McIntyre et al. 2004b).

During stimulation HF DBS seems to induce a regular bursting mode (Beurrier et al. 2002). After a reduction of stimulation artifacts, robust bursting activity in subthalamic nucleus (STN) neurons was observed in slices from naive or resperine-treated rats. After offset of stimulation, blockade of activity, i.e., a non-specific suppression of the neuronal activity in the target structures through a depolarization blockade which did not require synaptic transmission was observed (Beurrier et al. 2001).

Other hypotheses are that HF DBS applied to a PD patient mimics the effect of tissue lesioning and appears to block neuronal activity in relevant target areas during stimulation (Benabid et al. 2002). In single-compartment conductance-based biophysical models of isolated STN neurons the HF stimulation may cause a suppression of neuronal activity on an elementary membrane level, where a neuron's resting state or low-amplitude subthreshold oscillations can get stabilized (Pyragas et al. 2013). The obtained theoretical results resemble the clinically observed relations between stimulation amplitude and stimulation frequency required to suppress Parkinsonian tremor (Benabid et al. 1991). The most probable hypothesis was offered by Benabid et al. (2005), in which a mixture of different mechanisms was discussed. The contributing mechanisms resulting in the observed effects of HF DBS might be membrane inhibition, jamming, excitation of excitatory and inhibitory afferents, excitation of efferents and plasticity (Benabid et al. 2005). In particular, HF stimulation of afferent axons projecting to STN can account for a therapeutic effect of HF DBS within STN (Gradinaru et al. 2009).

To precisely evaluate the contribution of these different mechanisms, spatially extended multicompartment neuron models were used to demonstrate the effects of extracellular stimulation on the different structures of the stimulated neuronal population (Grill and McIntyre 2001). Depending on the stimulation amplitude and the shape of the stimulation pulses, either the cells were activated directly or fibers mediating excitatory or strong inhibitory action were activated (Grill and McIntyre 2001). Modeling studies indicate that already at the level of single neurons, the activation of a larger number of structures can take place with different and possibly conflicting impacts on the single neuron dynamics (Grill and McIntyre 2001). The collective dynamics of neuronal populations further adds aspects which are important for the creation of synchronized activity: cells responding differently to external inputs like somatosensory stimulation or stimulation due to active movements are present in the target tissue together with so called no-response cells (Lenz et al. 1994). HF stimulation has a complex impact on these structures (Benabid et al. 2002; Shen et al. 2003).

Experimental and modeling studies also indicate that the *globus pallidum interior* (GPi) – one structure of the basal ganglia – might be strongly involved in the mechanisms of DBS (Hashimoto et al. 2003; Garcia et al. 2005; McIntyre et al. 2004a; Rubin and Terman 2004; Miocinovic et al. 2006). The results of modeling studies indicate that under parkinsonian conditions the rhythmic inhibition from GPi to the thalamus compromises the ability of thalamocortical relay cells to respond to depolarizing inputs, such as sensorimotor signals. HF stimulation of STN regularizes GPi firing, and this restores the responsiveness of the thalamus (Rubin and Terman 2004). In such a way, one may distinguish between local and non-local effects of HF DBS. Locally, in the vicinity of the stimulation electrode, the axons rather than cell bodies (somas) get activated (McIntyre et al. 2004a), while the latter can even be effectively inhibited by the HF stimulation (Beurrier et al. 2001; Benabid et al. 2002; Welter et al. 2004; Meissner et al. 2005). The stimulation-induced axonal activity propagates antidromically and orthodromically (Hammond et al. 2008) and can change the firing

in the output structures downstream to the neuronal target population. The pathological discharge patterns there can be replaced by a HF spiking or suppressed depending on whether the efferent fibers of the stimulated nucleus are excitatory or inhibitory, respectively (Hashimoto et al. 2003; Anderson et al. 2003; McIntyre et al. 2004b). In other words, local and non-local effects of HF DBS may differ considerably.

HF DBS is reversible and has a much lower rate of side effects than lesioning with thermocoagulation (Schuurman et al. 2000). Although HF DBS is the golden standard for the therapy of medically refractory movement disorders, there are still limitations of HF DBS: On the one hand HF DBS may cause adverse effects like dysarthria, dysesthesia, cerebellar ataxia, and memory decline (Volkmann 2004; Rodriguez-Oroz et al. 2005; Freund 2005). On the other hand HF DBS may be ineffective or its therapeutic effect may wear off over time (Kumar et al. 2003; Rodriguez-Oroz et al. 2005). For instance, 11–15% of PD patients have unsatisfactory outcomes although their depth electrodes are properly placed (Limousin et al. 1999).

Coordinated Reset Stimulation

To study the impact of pulsatile stimuli on single oscillators and, in particular, populations of oscillators in a biologically more realistic setting, it was necessary to take into account random forces (Tass 1996a, b, 1999). To this end, a stochastic concept of phase resetting has been developed for populations of non-interacting (Tass 1996a, b) as well as interacting (Tass 1999) oscillators in the presence of noise. In this approach limit cycle oscillators were approximated by phase oscillators (Hansel et al. 1993b), so that the pulsatile stimulation only affects the oscillators' phases. If a single pulse of the right intensity and duration is delivered to the population in the stable synchronized state, it causes an at least temporary desynchronization provided it hits the population at a vulnerable phase. Theoretically, single pulse stimulation has also been studied in more complex networks, for instance, networks of coupled phase oscillators with inertia, modeling dendritic dynamics (Dolan et al. 2005; Majtanik et al. 2006). Based on the stochastic phase resetting theory and utilizing a phase oscillator as a model for a single neuron (Hansel et al. 1993b), demand-controlled single pulse deep brain stimulation has been suggested for the therapy of movement disorders like Parkinson's disease or essential tremor (Tass 1999, 2000).

However, there are drawbacks to single-pulse stimulation which decisively limit its applicability (Tass 2001b; Zhai et al. 2005): First, if the mutual coupling is not weak, the vulnerable phase range we have to hit in order to cause an effective desynchronization is only a small fraction (e.g., 5%) of a period of the collective oscillation. Second, the critical stimulation parameters required to achieve a good desynchronization depend on the initial dynamical state of the population. Thus, different stimulation parameters have to be used if the cluster is not in its stable synchronized state.

To overcome the limitations of single pulse stimulation, double pulse (Tass 2001a, b) stimulation has been proposed: Two qualitatively different stimuli are successively delivered. The first, stronger pulse resets (restarts) the collective oscillation irrespective of the initial state of the population. The second, weaker pulse is applied after a fixed time delay, where it hits the cluster in its vulnerable state and, hence, causes a desynchronization. There are different variants of double pulse stimulation, depending on the type of stimuli used to achieve a reset or a desynchronization (Tass 2001c, 2002a, b, c). For instance, the first resetting pulse can be replaced by a brief high-frequency pulse train (Tass 2001c) or by a softly resetting low-frequency pulse train (Tass 2002a, b).

Although double pulse stimulation causes a desynchronization irrespective of the initial dynamical state at which this stimulus is delivered, there are still limitations which may hinder an application to a biological system (Tass 2003a, b): On the one hand, double pulse stimulation requires a calibration. On the other hand, double pulse stimulation is only effective if the system parameters are reasonably stable. The required quasi-stationarity of the system parameters

combined with the possibly time consuming calibration may cause problems when applied to a real biological system, where fluctuations of model parameters are inevitable.

To provide a stimulation technique which is robust with respect to system parameters and which does not require calibration, coordinated reset (CR) stimulation has been developed (Tass 2003a, b). The idea behind this approach is to abstain from achieving a perfect desynchronization by a well-calibrated stimulus. Rather, by means of a robust and comparably mild stimulus the stimulated population is shifted into a dynamical state which is not the desired desynchronized state, but sufficiently close to it. Close in the sense that due to the pathologically strong coupling the population automatically relaxes into the desired desynchronized state. This approach essentially exploits the pathological tendency of the neuronal population to establish a synchronized state. Accordingly, CR stimulation is in a way comparable to Asian martial arts, where ideally a minimal amount of energy (i.e., CR stimulation) is invested to control the adversary by utilizing the adversary's own energy (i.e., the neurons' pathological strong coupling).

The scheme of the stimulation setup is presented in Fig. 3a. Several stimulation sites are placed within the target network and weak resetting stimulation signals are administered via these stimulation sites. In this way the oscillatory population is divided into several sub-populations, where each of them is assigned to the corresponding stimulation site and receiving the stimulation signal mostly from that stimulation site. CR stimulation means that a synchronized population of neurons is stimulated with a sequence of brief resetting stimuli (typically brief HF stimulus trains) via the different sites. The delay between the subsequent resetting stimuli can be chosen as $\tau = T/n$ with respect to that at the preceding site, where n is the number of stimulation sites, and T approximates the mean period of the collective dynamics of synchronized oscillators (Tass 2003a, b).

The subsequent reset of the different subpopulations induces a so-called cluster state, i.e., the whole population is divided into n subpopulations which differ with respect to their

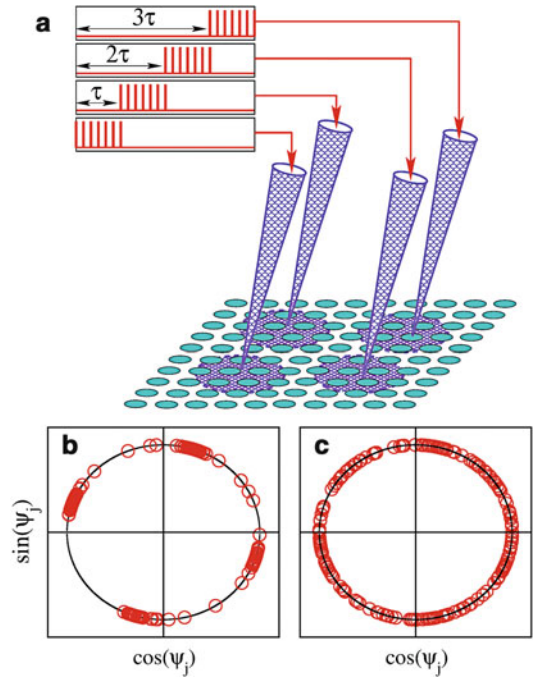

Brain Pacemaker, Fig. 3 Stimulation setup of CR stimulation method. (**a**) Brief and mild resetting stimuli are administered at different sites at subsequent times and effectively divide the stimulated population into several sub-populations such that (**b**) their phases ψ_j form phase clusters equidistantly (or close to that) distributed over the unit circle. (**c**) Nearly uniform distribution of the oscillator phases during the post-stimulation transient

mean phase. This effect is illustrated in Fig. 3b where a snapshot of the distribution of the phases ψ_j of stimulated oscillators is shown in the (cos(ψ_j),sin(ψ_j))-plane after CR stimulation. The phases of the population of oscillators stimulated via, e.g., four sites form four phase clusters distributed equidistantly (or close to that) over the unit circle. To estimate the extent and type of synchronization of the whole population of N oscillators, the cluster variables

$$Z_m(t) = R_m(t)\, e^{i\Psi_m(t)} = \frac{1}{N}\sum_{j=1}^{N} e^{i\, m\psi_j(t)}, \qquad (1)$$

can be used. $R_m(t)$ and $\Psi_m(t)$ are the corresponding real amplitude and real mean phase, where $0 \leq R_m(t) \leq 1$ for all time t (Daido 1992; Tass 1999). Cluster variables are convenient for characterizing synchronized states of

different types: Perfect in-phase synchronization corresponds to $R_1 = 1$, whereas an incoherent state, with uniformly distributed phases, is associated with $R_m = 0$, $m = 1, 2, 3, \ldots$ Small values of R_1 combined with large values of R_m are indicative of an m-cluster state consisting of m distinct and equally spaced clusters, where all oscillators within the same cluster have similar phases. In Fig. 3b, for instance, $R_1 \approx 0.02$, whereas $R_4 \approx 0.87$, indicating a four-cluster state induced by CR stimulation administered via four stimulation sites as in Fig. 3a.

From the cluster state the neurons typically relax to a uniformly desynchronized state (Fig. 3c) before they revert back to the in-phase synchronized state, if left unperturbed. To understand how a stimulus-induced clustering leads to an effective desynchronization, the dynamics of the leading modes $Z_1, Z_2, \ldots$, can be considered. When the coupling among oscillators becomes sufficiently large, e.g., it exceeds a certain critical value, Z_1 from (Eq. 1) becomes an *order parameter* (Kuramoto 1984), which according to the slaving principle (Haken 1983) governs the dynamics of the other stable modes Z_m ($m = 2, 3, \ldots$) on the center manifold (Pliss 1964): The order parameter Z_1 acts on a slow time scale, whereas the stable modes Z_m act on a fast time scale and relax to values given by the order parameter Z_1 (Wunderlin and Haken 1975; Haken 1983). In a system with a large number of oscillators this relationship reads (Tass 1999):

$$R_m \propto R_1^v \quad \text{with} \quad v \geq 2, \qquad m = 2, 3, 4, \ldots \tag{2}$$

Hence, to maintain a desynchronized neuronal firing, CR stimuli have to be administered repetitively.

CR stimulation exploits transient responses which are due to the oscillators' (pathologically strong) interactions. The general stimulation protocol of the intermittent CR stimulation is illustrated in Fig. 4. Here, the collective dynamics is

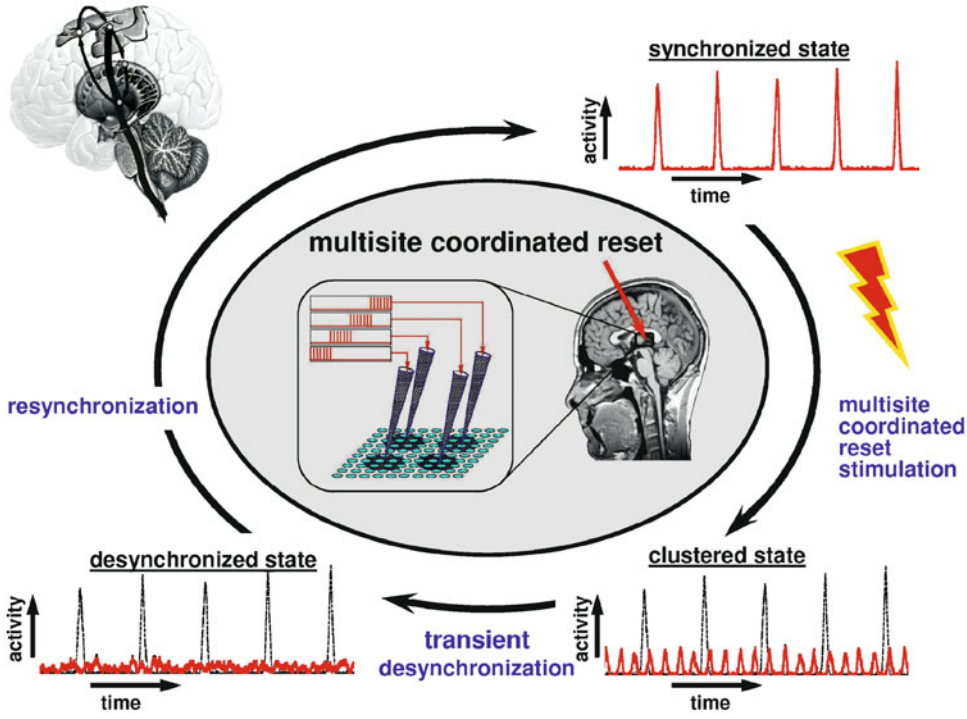

Brain Pacemaker, Fig. 4 A general scheme of the intermittent CR stimulation. Desynchronized firing of neurons is maintained by repetitive administration of CR stimuli intermingled with epochs of no stimulation

visualized by considering the collective firing of the neurons. A single firing/bursting model neuron fires/bursts whenever its phase is close to zero (modulo 2π) (Kuramoto 1984; Ermentrout and Kopell 1991; Grannan et al. 1993; Hansel et al. 1993a; Tass 1999). The collective firing can be illustrated with the *relative number of neurons producing an action potential or burst* at time t given by

$$n_{\mathrm{fire}}(t) = \frac{\text{number of neurons with } \cos\psi_j > 0.99}{N}. \tag{3}$$

$0 \leq n_{\mathrm{fire}}(t) \leq 1$ for all t. $n_{\mathrm{fire}}(t) = 0$ means that no neuron fires/bursts, while all neurons fire/burst at time t if $n_{\mathrm{fire}}(t) = 1$. Varying the threshold parameter 0.99 in a reasonable range does not change the results. As shown in Fig. 4, stimulation starts when the neurons are synchronized and the collective firing demonstrates high-amplitude rhythmic oscillations (upper-right insert in Fig. 4). After a few periods of stimulation the oscillatory population is set to a cluster state (bottom-right insert in Fig. 4). Then the stimulation is switched off and the ensemble returns to a synchronized state, on this way running through a uniformly desynchronized state (bottom-left insert in Fig. 4). And the procedure is repeated such that the ensemble is kept in a transient desynchronized state. The relaxation to a clustered state is due to the system being attracted by the center manifold as characterized by Eq. 2. By imposing a cluster state, the stimulation does only half of the desynchronizing work. The rest, namely approaching a uniformly desynchronized state, is done by the system itself. In this way the coupling, which causes the synchronization, is used for improving the desynchronizing effect. In the course of the post-stimulus transient R_1 and according to Eq. 2 also R_2, R_3, ... recover again. The system finally reaches its stable in-phase synchronized state again. In summary, by shifting the system into an unstable cluster state, the system reacts by automatically running through a desynchronized state. Finally, the system reverts back to the synchronized state, if left unperturbed.

The effectively desynchronizing intermittent CR stimulation can be used to block the resynchronization. For this, the repetitive stimulus administration can be organized either regardless of the state of the stimulated ensemble (open-loop control) or in a demand-controlled way (closed-loop control), where the following three different control strategies can be utilized:

(i) *Periodic administration of CR stimuli*: The most simple, open-loop type of stimulation is a periodic administration of CR stimuli. Here the time intervals of fixed length of CR stimulation (ON cycles) alternate with time intervals of fixed length where the stimulation is switched off (OFF cycles).

(ii) *Demand-controlled timing of the administration of identical stimuli*: Whenever the population tends to resynchronize, the same stimulus is administered (Fig. 5). The stronger synchronization among the neurons is, the more often a stimulus has to be administered to maintain an uncorrelated firing. In addition, for an ideal performance in an experimental application one has to observe the synchronized oscillation during a sufficiently long period of time in order to perform a frequency analysis which yields the period T of the population in the absence of stimulation and, thus, the critical stimulation parameter τ (the time delay between the two successive HF pulse trains administered via different stimulation sites, see Fig. 3). Moreover, instead of performing such a calibration of, pre-set values of can be used by adapting the latter to the typical frequency range of the pathological oscillation (see, e.g., Tass et al. 2012b).

(iii) *Periodically administered HF pulse trains of demand-controlled length*: The stimuli are periodically administered with offset times $t_k = kvT$, where $k = 0, 1, 2, 3, \ldots$ is the index labeling the different stimuli, $T = \tilde{T} + \varepsilon$ is a time interval in the range of the period $\tilde{T}$ of the population without stimulation, and v is a small integer such as 2 or 3. This means that a 1:v entrainment of the four sub-populations is performed, where the spontaneous

frequency of the neurons is approximately v times larger compared to the frequency of stimulus administration. The smaller $|\varepsilon|$, the smaller is the stimulation strength necessary to achieve an entrainment.

The closed-loop variants (*ii*) and (*iii*) require that the ensemble's activity or at least a quantity representing the extent of synchronization can be measured appropriately. Here, either the start times of identical CR stimuli or the length of periodically administered stimuli are calculated from the values of R_1. For example, in the case (*ii*) the stimulation is started if R_1 becomes larger than a certain threshold (Fig. 5, upper two plots), whereas in the case (*iii*) the stimulation period is longer for larger values of R_1 measured at the onset of the stimulation (Fig. 5, bottom two plots). In the latter case the length of the HF pulse trains increases linearly between a minimal value $M_{\min}$ and a maximal value $M_{\max}$ of single-pulses (except for rounding), where the latter is initially used for desynchronizing the fully synchronized population. R_1 is measured at (or, in practice, close to) times $t'_k = t_k - t_{\max}$ where $t_{\max}$ the maximal duration of a HF pulse train (containing $M_{\max}$ single-pulses). $R_1(t'_k)$ determines the number of pulses of the HF pulse trains administered via each of the stimulation sites of the kth stimulus according to

$$M_k = \min\left\{\left[\frac{R_1(t'_k)(M_{\max} - M_{\min})}{R_1(t_0)}\right]_{\mathbb{Z}} + M_{\min}, M_{\max}\right\}, \tag{4}$$

where $k = 0, 1, 2, 3, \ldots$, $[x]_{\mathbb{Z}}$ stands for rounding x to the nearest integer, and min $\{x_1, x_2\}$ stands for the minimum of $\{x_1, x_2\}$. The kth stimulus ends precisely at time $t_k = kvT$, whereas it starts somewhere between t'_k (for $M_k = M_{\max}$) and t_k (for $M_k = M_{\min} = 0$), depending on its duration. If the suppression of R_1 is not sufficient one may (i) choose a larger intensity of

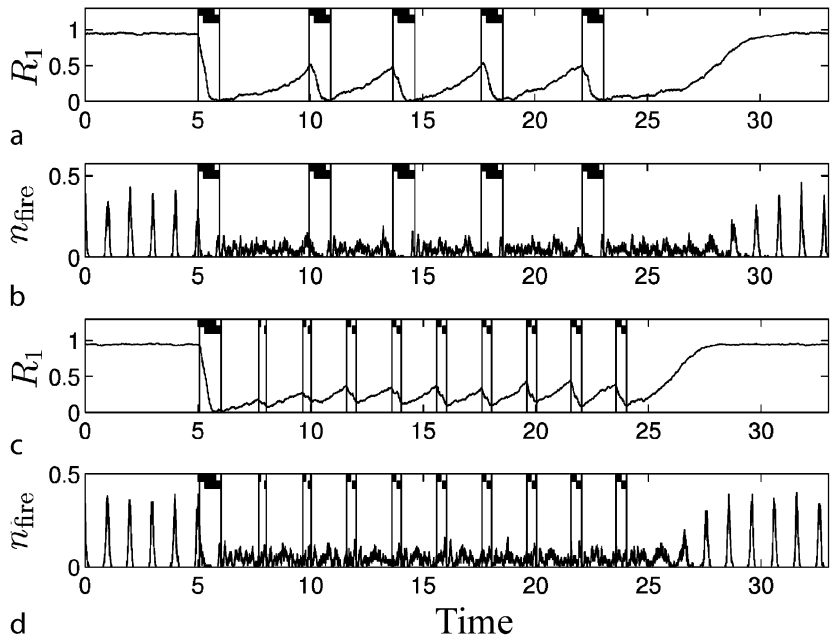

Brain Pacemaker, Fig. 5 Desynchronizing effect of the demand-controlled intermittent CR stimulation. Time course of R_1 from Eq. 1 (**a** and **c**) and of n_{fire} from Eq. 3 (**b** and **d**) during different types of stimulation. *Demand-controlled timing of stimulus administration* (**a** and **b**): As soon as the amplitude R_1 of the recovering order parameter reaches the value of 0.5, the stimulus is administered again. *Periodical stimulation with demand-controlled length of HF pulse train* (**c** and **d**): The stimulus is administered periodically, where the length of the HF pulse trains is adapted to R_1 according to Eq. 4 with $M_{\max} = 15$ and $M_{\min} = 0$. First published in Tass (2003b)

stimulation, (ii) increase $M_{\min}$, (iii) administer the stimuli at a higher rate, i.e. decrease ν, so that the inter-stimulus interval $t_{k+1} - t_k = \nu T$ gets smaller, (iv) increase the duration of each single pulse of the pulse trains and/or increase the intra-burst frequency of the pulse trains (i.e., bursts). The feedback value of R_1 can also be evaluated before time t'_k, especially in case of a slow order parameter dynamics (i.e., when the synchronization is weak with respect to the noise). One could also use the mean of R_1 in a period of evaluation.

Applying the standard, permanent HF stimulation (Benabid et al. 1991; Blond et al. 1992) (in a first approximation) corresponds to stimulating each neuron with the same HF pulse train. During a permanent HF stimulation a high-frequency entrainment of the order parameter Z_1 captures Z_1 in a small portion of the complex plane (Tass 2001c), so that the individual neurons' firing is stopped, but no desynchronization occurs. In contrast, during stimulation R_1 can be even larger compared to its pre-stimulus level, and after stimulation the synchronous firing continues immediately. To suppress the firing with such a simple pulse train persistently, it has to be administered permanently. The number of single pulses used to suppress the firing in the case of the standard permanent HF pulse train stimulation is about five to eight times larger than that used for blocking the resynchronization in Fig. 5a–d, respectively. This illustrates the effectiveness of the demand-controlled CR stimulation. The latter can effectively desynchronize stimulated oscillators with a significantly smaller amount of stimulation current compared to the standard permanent HF pulse-train stimulation.

The efficacy of CR stimulation can further be improved by an optimal choice of stimulation parameters. Several computational studies on neuronal models of different complexity have addressed this problem and showed that the intermittent m: n ON–OFF CR stimulation, where m cycles with stimulation ON are recurrently followed by n cycles with stimulation OFF, is most effective for a weak stimulation intensity and short ON intervals (Lysyansky et al. 2011a). The stimulation-induced cluster state leads to the longest desynchronizing post-stimulation transient which can further be prolonged for non-uniform timing of the stimuli onsets (Luecken et al. 2013). The number of stimulation sites is another important stimulation parameter, and its optimal choice essentially depends on the properties of the neuronal tissue (Lysyansky et al. 2013). For a weak (strong) spatial decay rate of the stimulation current with distance to the stimulation site, CR stimulation can optimally be delivered via small (large) number of stimulation sites.

The theoretical findings on the properties of CR stimulation have been verified experimentally. The resetting impact and the induced transient desynchronization of an electrical short-pulse stimulation, on which the CR technique is based, have been reported *in vivo* for coupled neuronal bursters in paddle fish (Neiman et al. 2007). Taking into account the spike timing-dependent synaptic plasticity (see section "Plasticity"), the long-lasting desynchronizing effects of CR stimulation have been investigated in detail in theoretical studies (Tass and Majtanik 2006; Tass and Hauptmann 2006, 2007; Hauptmann and Tass 2007), and the results have been confirmed experimentally *in vitro* in rat hippocampal slice (Tass et al. 2009). The beneficial therapeutic long-lasting aftereffects of weak CR stimulation have been observed in the 1-methyl-4-phenyl-1,2,3,6-tetrahydropyridine (MPTP)-treated macaque monkeys in contrast to a stronger CR stimulation and to the standard HF DBS (Tass et al. 2012b).

Modeling shows that CR stimulation can be effective for a number of stimulation setups and demonstrate a great applicability. Based on a computational study, CR stimulation has been suggested for counteraction of cerebral hypoactivity, in particular, to activate hypo-active or inactive neuronal populations found in a number of diseases without promoting pathological synchronization by a multi-frequency and phase-shifted activation of the stimulated neuronal networks (Lysyansky et al. 2011b). Other computational studies showed that CR stimulation can be effective in inducing desynchronization for direct somatic stimulation and as well as for excitatory or inhibitory synaptically meditated stimulation (Popovych and Tass 2012). The latter stimulation

setup might correspond to stimulation of afferent or efferent fibers or sensory stimulation where the stimulation signals arrive at the neural target population as post-synaptic potentials. Sensory CR stimulation has been suggested for suppression of the neural synchrony underlying tinnitus (Tass and Popovych 2012) and successively verified in a clinical proof of concept study in tinnitus patients treated with non-invasive acoustic CR stimulation (Tass et al. 2012a; Silchenko et al. 2013; Adamchic et al. 2013).

Multisite Linear Delayed Feedback

Similarly as in the case of CR stimulation, multisite linear delayed feedback (MLDF) (Hauptmann et al. 2005a, b, c, 2007a) is administered via several stimulation sites, e.g., via four sites as illustrated in Fig. 3a. The individual stimulation signals $S_m(t)$ of each of the stimulation sites are however derived from the delayed mean field $Z(t)$ of the stimulated ensemble using different time delays for different stimulation signals. The mean field characterizes the collective macroscopic dynamics of the oscillators and can be viewed as the ensemble average of the signals $z_j(t)$, $j = 1, \ldots, N$, of individual oscillators, $Z(t) = N^{-1} \sum_{j=1}^{N} z_j(t)$.

For n stimulation sites, the stimulation signals are calculated as $S_m(t) = KZ(t - \tau_m)$, $m = 1, \ldots, n$, where K is the amplification parameter, and the values of delay τ_m, for example, for $n = 4$ are calculated from the following relation:

$$\tau_m = \frac{11 - 2(m-1)}{8}\tau, \quad m = 1, 2, 3, 4. \qquad (5)$$

The delays τ_m are symmetrically distributed with respect to the main delay τ, where the smallest time delay between neighboring stimulation sites is chosen as $\tau/4$. In the case $\tau = T$ (mean period of the ensemble), the delays τ_m are uniformly distributed over the mean period T. In another realization, instead of four delays τ_m, $m = 1, \ldots, 4$ one can use only two of them, e.g., τ_1 and τ_2. One can put $\tau_3 = \tau_1$ and $\tau_4 = \tau_2$, where the polarity of the stimulation signals $S_3(t)$ and $S_4(t)$ is reversed: $S_3(t) = -S_1(t)$ and $S_4(t) = -S_2(t)$. Assuming that the mean field of the ensemble uniformly oscillates with period $T = \tau$, the alternating polarity of the signal corresponds to a shift in time by half a period. Therefore, under this condition the stimulation signal $S_3(t) = -S_1(t) = -KZ(t - \tau_1)$ approximates the stimulation signal $S_1(t + \tau/2)$ which is shifted in time by half of the period, which, in turn, is equal to $KZ(t - \tau_3)$, where τ_3 is calculated according to Eq. 5. Analogous arguments are applicable to the stimulation signal $S_4(t) = -S_2(t) = -KZ(t - \tau_2)$.

If the phase $\Psi(t)$ of the mean field $Z(t)$ (see also Z_1 from Eq. 1) uniformly rotates with a constant frequency $\Omega = 2\pi/\tau$, the phases $\Phi_m(t) = \Psi(t - \tau_m)$ of the stimulation signals $S_m(t)$ are distributed uniformly over the unit circle as illustrated in Fig. 6a. Then the phases $\psi_j(t)$ of the stimulated neuronal subpopulation assigned to the stimulation site m are attracted to the phase $\Psi(t - \tau_m)$ of the corresponding stimulation signal. Hence, the phases of all oscillators stimulated with MLDF become symmetrically redistributed on the circle $(0, 2\pi)$ in a cluster state. The order parameter $R_1(t)$ thus gets minimized. Depending on the value of delay τ, the stimulation can induce different clustered states in the stimulated ensemble, where the corresponding order parameter R_m attains large values.

As shown in Fig. 6b, c, the in-phase synchronization in the stimulated ensemble is effectively suppressed (for time $t > 200$, where both coupling and stimulation are switched on), where the order parameter $R_1 = |Z_1(t)|$ from Eq. 1 attains small values (Fig. 6b, c, *red curve*). This indicates a symmetrical redistribution of the oscillator phases $\psi_j(t)$ over the unit circle. For the parameter τ close to the mean period T of the stimulation-free ensemble a four cluster state is induced by the stimulation, where the order parameters R_1 and R_2 are small, whereas R_4 is relatively large (Fig. 6b). In the subplot, where four trajectories from each of the stimulated subpopulations are depicted, the emerging four-cluster state induced by MLDF is illustrated. For τ closer to, for example, $2T$ the stimulation

induces a two-cluster state, where R_1 is small, whereas R_2 and R_4 are large (Fig. 6c). The oscillators thus split into two clusters, which is also illustrated in the subplot in Fig. 6c.

MLDF robustly suppresses the in-phase synchronization as shown in Fig. 7a, where the time-averaged order parameter $\langle R_1 \rangle$ attains small values for a broad range of parameters τ and K. On the other hand, depending on system and stimulation parameters, MLDF can induce either a two-cluster state, where the second order parameter R_2 attains relatively large values (e.g., for $\tau \approx 2T$, see Fig. 7b), or a four-cluster state, where R_2 becomes small and the fourth order parameter R_4 increases (e.g., for $\tau \approx T$, see Fig. 7c). Therefore, the whole stimulated population is divided into two or four distinct sub-populations. Within the phase clusters the individual oscillators have phases close to each other, while the different phase clusters are equidistantly distributed within the cycle. Hence, depending on the values of the parameters τ and K, MLDF with four stimulation sites may cause either a two-cluster state, where R_1 is close to zero and R_2 is large, or a four-cluster state, where both R_1 and R_2 are small, but R_4 is large. The cluster states become less pronounced and the phases redistribute on the circle even more uniformly if a local coupling as well as spatially decaying profile of the current spread is taken into account (Hauptmann et al. 2005a).

In Fig. 7d a similar two-parameter diagram for the averaged order parameter $R_1(t)$ is presented for a *single-site linear delayed feedback* (SLDF) suggested for synchronization control in references (Rosenblum and Pikovsky 2004a, b). The stimulation is performed via one stimulation electrode in such a way that all oscillators of the

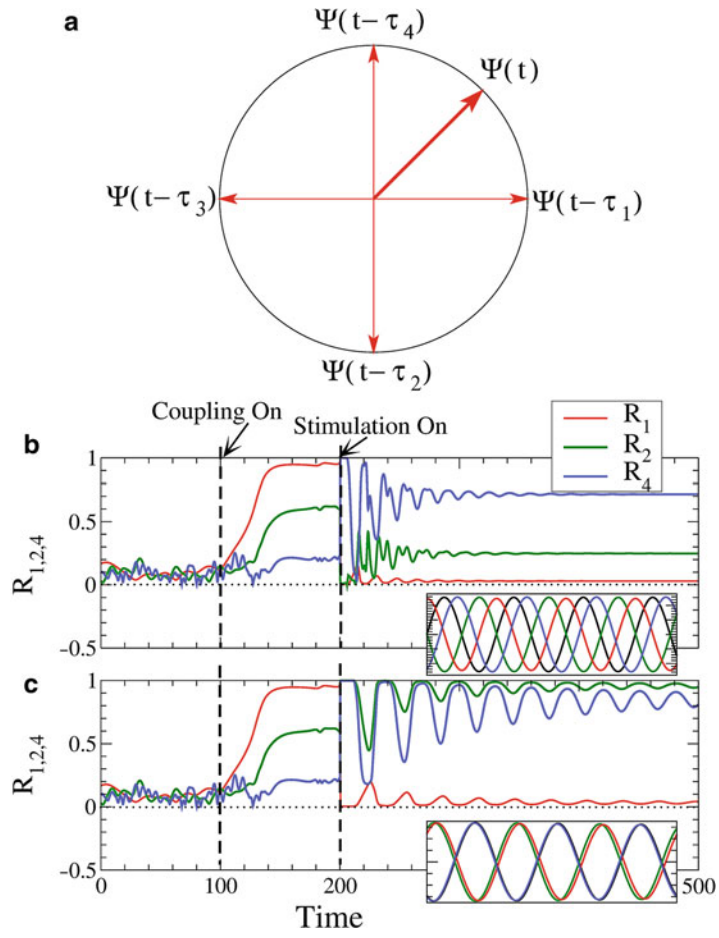

Brain Pacemaker, Fig. 6 Control of synchronization by multisite linear delayed feedback (MLDF) stimulation. (**a**) Distribution of the phases $\Phi_m(t)$ of the stimulation signals $S_m(t)$ administered via four stimulation sites (as in Fig. 3a), which are the delayed mean phase, $\Phi_m(t) = \Psi(t - \tau_m)$, with delays τ_m from Eq. 5 for $\tau = T$. (**b** and **c**) Time courses of the amplitudes of the cluster variables (Eq. 1), the order parameters R_1, R_2 and R_4. In the subplots four trajectories from each of four stimulated sub-populations assigned to each of four different stimulation sites are shown for $t \in (320,340)$. Parameter $\tau = T$ in (**b**) and $\tau = 2T$ in (**c**)

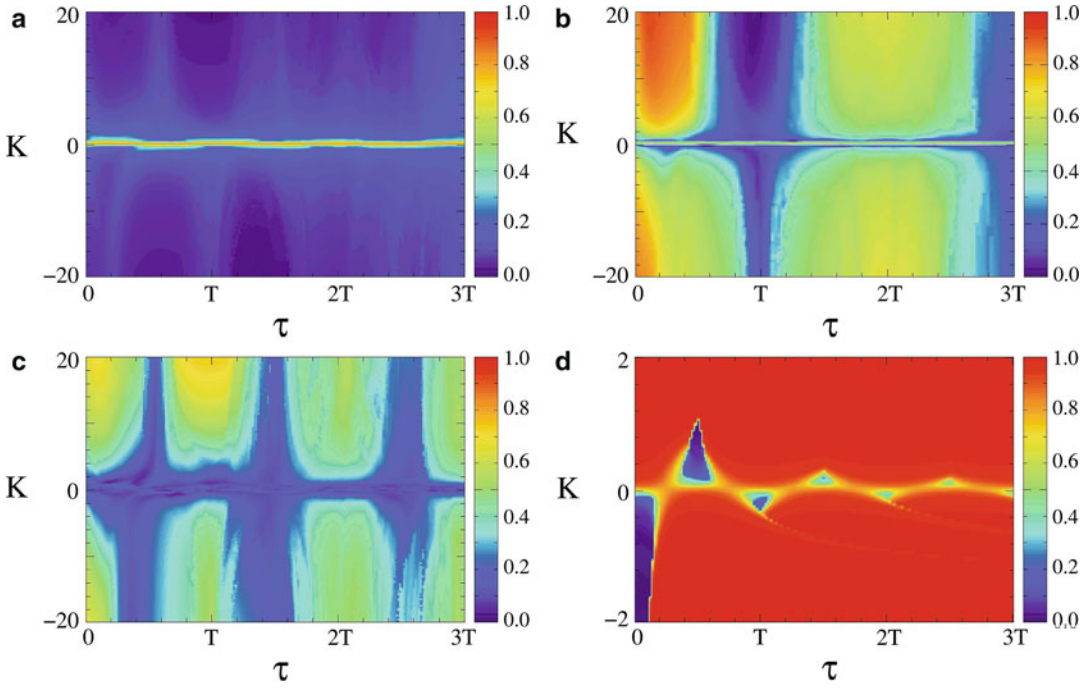

Brain Pacemaker, Fig. 7 Impact of the MLDF stimulation versus parameters τ and stimulus amplification K. The time-averaged order parameters $\langle R_1 \rangle$, $\langle R_2 \rangle$, and $\langle R_4 \rangle$ are depicted in plots (**a–c**), respectively, and encoded in color ranging from 0 (*blue*) to 1 (*red*). In plot (**d**) the impact of the single-site linear delayed feedback (SLDF) on the oscillatory population is illustrated, where the values of the order parameter $\langle R_1 \rangle$ are depicted in color versus parameters τ and K (First published in Popovych et al. (2006a))

ensemble (in the first approximation) receive the same stimulation signal $S(t)$. In this case the stimulation signal $S(t)$ attains the form $S(t) = KZ(t - \tau)$. For the stimulation with SLDF, in the corresponding two-parameter diagram (Fig. 7d) islands of perfect desynchronization are complemented by areas of stimulation-enhanced synchronization. In the limit $N \to \infty$ the order parameter $R_1 = 0$ in the desynchronization regions, where the phases are uniformly distributed on the circle $(0, 2\pi)$ (Rosenblum and Pikovsky 2004a, b). This is the state of complete desynchronization, where the stimulated oscillators rotate with different frequencies indicating an absence of any clustered state whatsoever. The island-like structure of desynchronization regions in parameter space of SLDF (Fig. 7d) was also experimentally confirmed for arrays of coupled electrochemical oscillators (Zhai et al. 2008).

The important property of the stimulation with the multi- and single-site linear delayed feedback is the inherit demand-controlled character of the methods. As soon as the desired desynchronized state is achieved, the values of the order parameter $R_1(t)$, i.e., the amplitude of the mean field become small. Along with the order parameter, in the desynchronized state the amplitude of the stimulation signal $S(t)$ vanishes as well. The stimulation with multi- and single-site linear delayed feedback thus represents noninvasive control methods for desynchronization of coupled oscillators. The stimulated ensemble is then subjected to a highly effective control at a minimal amount of stimulation force.

Nonlinear Delayed Feedback

As for the case of the single-site linear delayed feedback, for the stimulation with nonlinear delayed feedback (NDF) only one registering and one stimulating site is required, see Fig. 8a. All stimulated oscillators receive the same stimulation signal $S(t)$ which is constructed from the

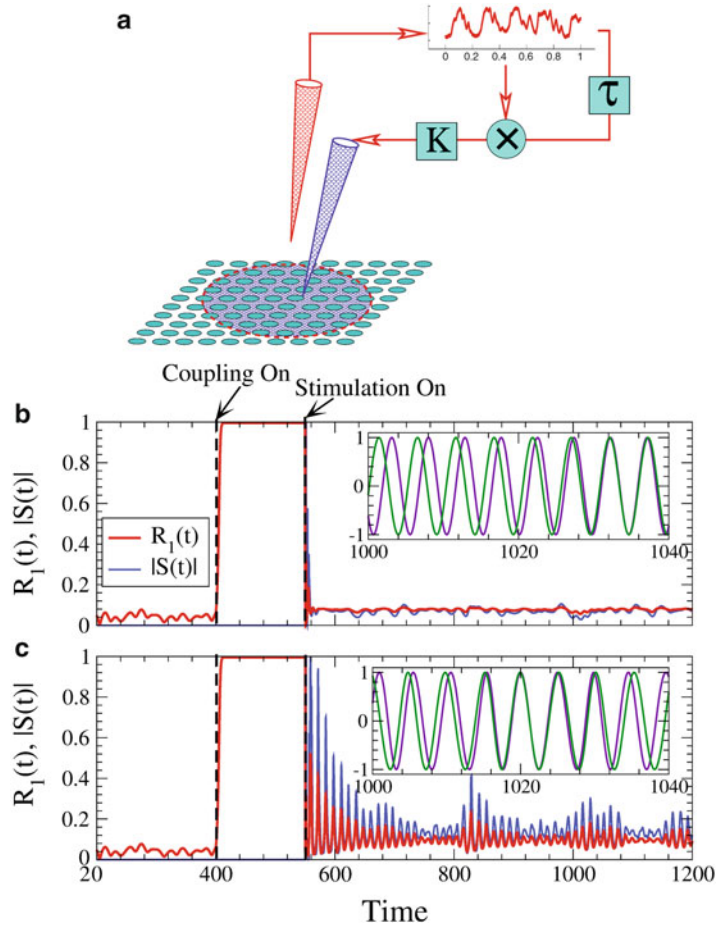

Brain Pacemaker, Fig. 8 Control of synchronization by nonlinear delayed feedback (NDF) stimulation. (**a**) The macroscopic activity (mean field) of the controlled population is measured, delayed, nonlinearly combined with the instantaneous mean field, amplified, and fed back via a single stimulation site. (**b** and **c**) Desynchronization of strongly synchronized oscillators by NDF. Time courses of the order parameter $R_1(t)$ (*red curves*) and the amplitude of the stimulation signal $|S(t)|$ (*blue curves*) are plotted for delay (**b**) $\tau = T/2$ and (**c**) $\tau = T$, where T is the mean period of the stimulation-free ensemble. In the subplots trajectories of two selected oscillators are depicted in the stimulated regime (First published in Popovych et al. (2008))

measured mean field of the ensemble. It is assumed that the measured mean field $Z(t)$ of the ensemble has the form of a complex analytic signal $Z(t) = X(t) + iY(t)$, where $X(t)$ and $Y(t)$ are the real and imaginary parts of $Z(t)$, respectively. If only a real part $X(t)$ of the mean field is measured, the imaginary part can be calculated, e.g., with the help of the Hilbert transform (Pikovsky et al. 2001). The stimulation signal is then constructed by a nonlinear combination of a delayed complex conjugate mean field with the instantaneous mean field (Popovych et al. 2005, 2006a, b; Tass et al. 2006),

$$S(t) = KZ^2(t)Z(t-\tau), \tag{6}$$

where K is a stimulus amplification parameter, τ is a time delay, and the asterisk denotes complex conjugacy.

The desynchronizing effect of the stimulation with NDF is illustrated in Fig. 8b, c. The onset of stimulation at $t = 550$ results in desynchronization of the stimulated oscillators and the order parameter $R_1(t)$ reaches the values of approximately the same order of magnitude as in the uncoupled regime ($t < 400$). This indicates a high level of desynchronization. The stimulation does not destroy the normal oscillatory activity of the individual oscillators. In the insets in Fig. 8b, c individual trajectories of two selected oscillators of stimulated ensemble are plotted. The stimulated oscillators rotate with different individual frequencies just as in the coupling- and stimulation-free regime.

As soon as a desynchronized state is achieved, the stimulation force declines and the stimulated system is subjected to a highly effective control with a minimal amount of stimulation force. Also,

as soon as a resynchronization occurs, the mean field starts to exhibit large-amplitude oscillations and the stimulation signal increases its amplitude and brings the ensemble back to a desynchronized state. This demand-controlled character of the nonlinear delayed feedback is illustrated in Fig. 8c where the onsets of resynchronization (increase of $R_1(t)$, *red curve*) at times around $t \approx 850$, 1,050, and 1,200 lead to an increase of the amplitude of the stimulation signal $|S(t)|$ (*blue curve*), which in turn results in a suppression of the resynchronization.

The impact of the nonlinear delayed feedback on the stimulated oscillators is twofold. On one hand, the stimulation can effectively desynchronize even strongly interacting oscillators for a large range of the stimulus amplification K, see Fig. 9a. This effect is very robust with respect to the variation of the delay τ and, as a result, with respect to the variation of the mean frequency Ω of the stimulated ensemble. On the other hand, in a weakly coupled ensemble the stimulation can induce synchronization in island-like regions of small values of the stimulus amplification K complemented by domains of desynchronization, see Fig. 9b.

An increase of the stimulus amplification parameter K results in a gradual decay of the order parameter R_1 for both strongly and weakly coupled oscillators, which indicates an onset of desynchronization in the stimulated ensemble. Simultaneously, the amplitude of the stimulation signal $|S(t)|$ decays as well, indicating the demand-controlled character of the nonlinear delayed feedback stimulation. For a fixed delay $\tau > 0$ the order parameter and the amplitude of the stimulation signal decay as $|K|$ increases according to the following power law (Fig. 10a):

$$R_1 \sim |K|^{-1/2}, \qquad |S| \sim |K|^{-1/2}. \tag{7}$$

The desynchronization transition for increasing K also manifests itself in a sequence of frequency-splitting bifurcations, where the observed individual frequencies $\overline{\omega}_j = \left\langle \dot{\psi}_j \right\rangle$ of the stimulated oscillators split, one after another from the mean frequency Ω as K increases (Fig. 10b) and approach the natural frequencies of the unperturbed oscillators (Fig. 10b, *blue diamonds*). For large values of K all stimulated oscillators rotate with different frequencies close to the natural frequencies ω_j. The oscillators thus exhibit a uniform desynchronous dynamics without any kind of cluster states. In addition, depending on the values of the delay τ, the nonlinear delayed feedback can significantly change the mean frequency Ω, i.e., the frequency of the mean field $Z(t)$ of the stimulated ensemble (Popovych et al. 2005, 2006a). The macroscopic dynamics can thus be either accelerated or slowed down, whereas the individual dynamics remains close to the original one. This opens an approach for the frequency control of the oscillatory population stimulated with the nonlinear delayed feedback.

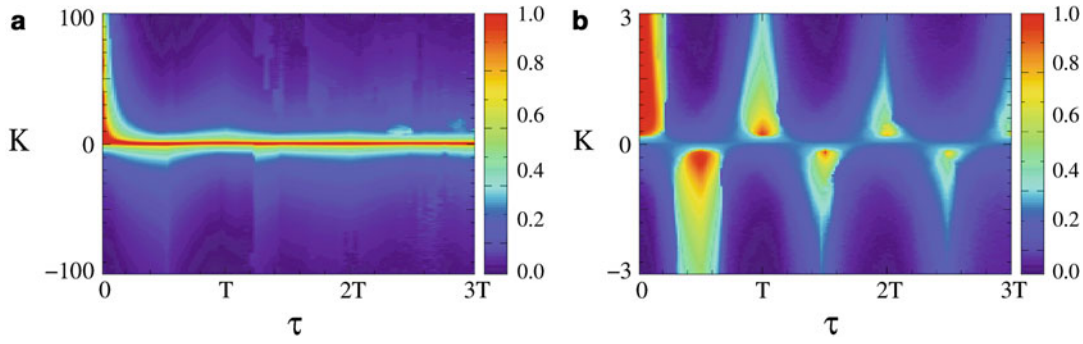

Brain Pacemaker, Fig. 9 Robustness of the NDF effects. (**a**) Stimulation-induced desynchronization and (**b**) stimulation-induced synchronization in ensembles of (**a**) strongly coupled and (**b**) weakly coupled oscillators. The time-averaged values of the order parameter R_1 are encoded in color ranging from *red* (synchronization) to *blue* (desynchronization) versus delay τ and stimulus amplification K

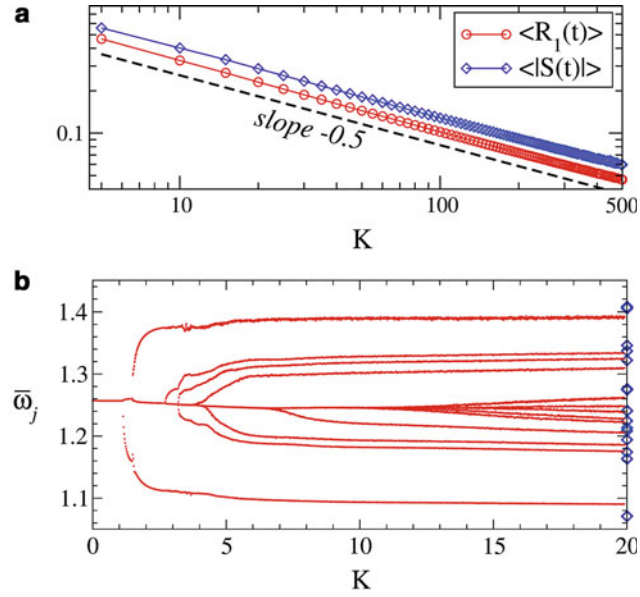

Brain Pacemaker, Fig. 10 Impact of NDF as the stimulus amplification K increases. (**a**) Log–log plot of the time-averaged order parameter R_1 and amplitude of the stimulation signal $|S(t)|$ versus K. The *dashed line* has the slope −0.5 and is given for comparison. (**b**) The observed individual frequencies $\overline{\omega}_j$ of the stimulated oscillators versus K. *Blue diamonds* at the right vertical axis depict values of the natural frequencies of the oscillators (First published in Popovych et al. (2006a))

Mixed Nonlinear Delayed Feedback

The NDF method can also be applied for desynchronization and decoupling of two (or more) interacting oscillator populations. For this, the mixed NDF can be used (Popovych and Tass 2010), see Fig. 11a. For a drive-response coupling scheme, the coupling within population 2 is assumed to be weak, so that, being isolated from population 1, no synchronization emerges in population 2. In contrast, the coupling in population 1 is strong enough to cause synchronization within population 1. It then drives the second population, which synchronizes because of the driving and sends a response signal back to population 1. The second ensemble is stimulated with signal $S(t)$, which is constructed from the mixed mean field Z_ε according to the rule of NDF from Eq. 6. The mixed mean field $Z_\varepsilon = \varepsilon W_1 + (1 - \varepsilon)W_2$ is a linear combination of the mean fields W_1 and W_2 of populations 1 and 2, respectively.

The level of mixing of the mean fields W_1 and W_2 within the stimulation signal is given by the parameter ε. Depending on it the mixed NDF can have different desynchronizing effects on populations 1 and 2.

- *Small* ε: mostly population 2 contributes to the stimulation signal. The mixed NDF desynchronizes the driven and stimulated population 2 (Fig. 11b), but the driving ensemble 1 remains unaffected and exhibits strongly synchronized dynamics (Fig. 11c). The populations get effectively decoupled from each other.
- *Intermediate* ε: both populations equally contribute to the stimulation signal. Both ensembles remain synchronized (Fig. 11b, c).
- *Large* ε: mostly population 1 contributes to the stimulation signal. Both ensembles are effectively desynchronized by the mixed NDF (Fig. 11b, c).

In the latter case the desynchronization induced by the mixed NDF in the driven and stimulated population 2 propagates to the drive population 1 which is not directly stimulated. This is indicative of an indirect control of synchronization by the mixed NDF.

Proportional–Integro–Differential Feedback

For a particularly difficult situation, where the measurement and stimulation are not possible at the same time and at the same place, there is another control method which is based on a proportional–integro–differential feedback (PIDF). The scheme of this stimulation protocol is sketched in Fig. 12a, see also Fig. 11a for $\varepsilon = 1$ except for the

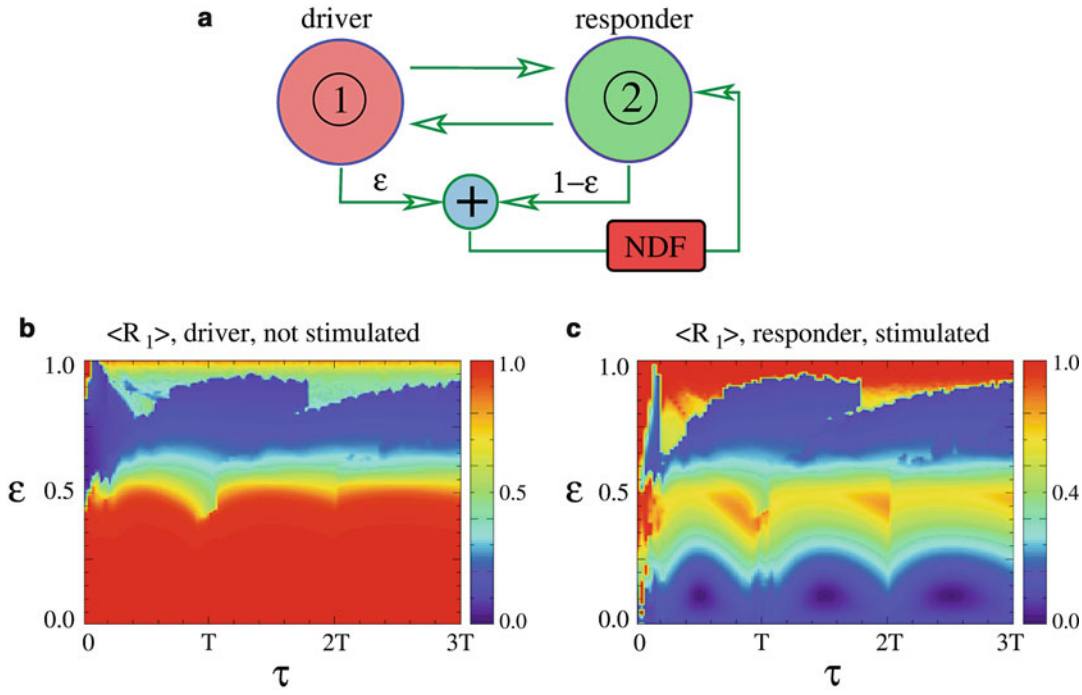

Brain Pacemaker, Fig. 11 Desynchronization and decoupling of interacting populations by the mixed NDF. (**a**) Stimulation setup: The measured mean fields of populations 1 and 2 is linearly combined into a mixed mean field, processed by the NDF algorithm (Eq. 6), and fed back to the target population 2. (**b** and **c**) Time-averaged order parameter R_1 of (**b**) intrinsically synchronized, drive population 1 and (**c**) stimulated population 2 driven to synchronization by population 1 versus time delay τ and mixing parameter ε. The *color coding* as in Fig. 9 (First published in Popovych and Tass (2010). Copyright (2010) by the American Physical Society)

measured signal being processed by a PIDF algorithm. The controlled ensemble of N coupled oscillators is divided into two separate sub-populations of N_1 and $N_2 = N - N_1$ oscillators, one being exclusively measured and the other being exclusively stimulated. In this way a separate stimulation-registration setup is realized, where the recording and stimulating sites are spatially separated and the measured signal is not corrupted by stimulation artifacts. The observed signal is considered to be the mean field W_1 of the measured sub-population. Below the main attention will be paid to the proportional-differential (PD) feedback only (for more details, see Pyragas et al. (2007)). Then, the stimulation signal $S(t)$ administered to the second, stimulated sub-population is constructed as

$$S(t) = PW_1(t) + D\dot{W}_1(t), \qquad (8)$$

where the parameters P and D define the strength of the proportional and differential feedback, respectively. The effect of the stimulation with PD feedback is illustrated in Fig. 12b. As the strength of the feedback (parameters P and D) increases the stimulation results in a complete desynchronization of the whole ensemble. The threshold of the onset of desynchronization depends on the relative splitting $N_1 : N_2$ of the oscillators between sub-populations and on the mean frequency Ω: The threshold is larger for smaller number of oscillators N_2 in the stimulated populations or for larger frequency Ω. The later dependence can be eliminated if an integral component is included in the stimulation signal, see Pyragas et al. (2007). Moreover, if the coupling in the ensemble is rather weak, the desynchronization can be achieved by applying the proportional feedback only. In contrast, in the case of strong coupling the stimulation signal additionally requires the differential feedback for robust desynchronization. As illustrated in the two-parameter diagrams in Fig. 12c, d, there exists a certain threshold in parameters P and D values, where the stimulation with PIDF

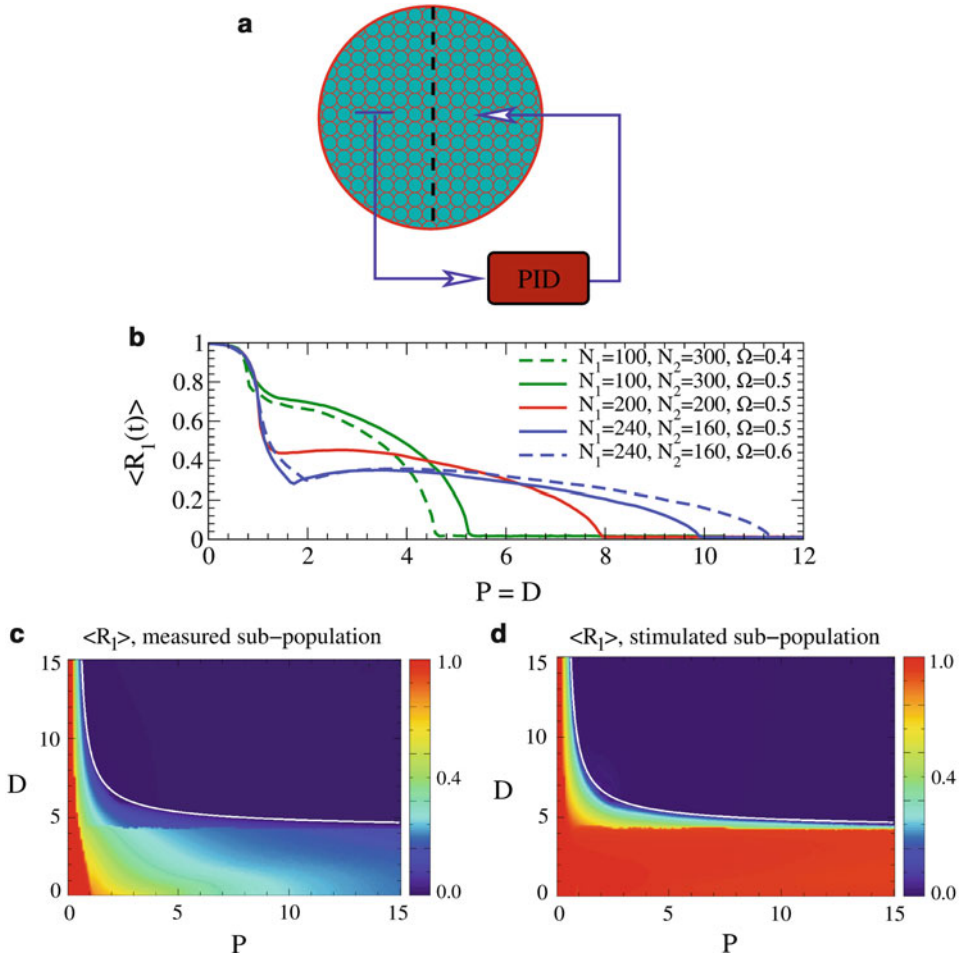

Brain Pacemaker, Fig. 12 PIDF control: (**a**) The mean field is measured in one part of the controlled ensemble and, after processing according to proportional–integro–differential feedback (PIDF) algorithm, is administered to the other part of the ensemble. (**b**) The time-averaged order parameter R_1 of the whole ensemble versus the strength of the PD feedback (with $P = D$) for different splitting $N_1 : N_2$ and different mean frequencies Ω. (**c** and **d**) The time-averaged order parameters R_1 (encoded in *color*) of (**c**) the measured sub-population and (**d**) stimulated sub-population versus stimulation parameters P and D. The *white curve* is the parameter threshold for the onset of desynchronization in the sub-populations (First published in Pyragas et al. (2007). Used with permission from EPL)

desynchronizes both sub-populations in the target ensemble: stimulated sub-population (Fig. 12c) and also measured, non-stimulated sub-population (Fig. 12d). In this sense the PIDF stimulation method appears to be very effective even for a complicated stimulation protocol with a separate stimulation-registration setup.

Plasticity

Plasticity is a fundamental property of the nervous system: In order to learn and to adapt to sensory inputs, neurons continuously adapt the strength of their synaptic connections in relation to the mutual timing properties of their firing or bursting (Hebb 1949; Gerstner et al. 1996; Markram et al. 1997; Debanne et al. 1998; Kilgard and Merzenich 1998; Abbott and Nelson 2000; Feldman 2000; Song et al. 2000; van Hemmen 2001; Zhou et al. 2003). However, plasticity may not only lead to desired learning and optimization processes. Rather neuronal populations can learn pathologically strong interactions which may lead, e.g., to the emergence of epilepsies

(Morimoto et al. 2004; Speckmann and Elger 1991). This is well-known from the so-called kindling phenomenon (Goddar 1967), where preparatory stimulation induces the spontaneous production of epileptic seizures without gross morphological changes (Morimoto et al. 2004).

The impact of plasticity on synaptic weights and collective neuronal dynamics has been accounted for by several theoretical studies on desynchronizing stimulation methods (Tass and Majtanik 2006; Hauptmann and Tass 2007; Tass and Hauptmann 2007; Maistrenko et al. 2007). They have initiated an approach which aims at unlearning pathologically strong synaptic interactions by desynchronizing brain stimulation and which has further been developed in latter papers (Hauptmann and Tass 2009, 2010; Tass and Popovych 2012; Popovych and Tass 2012). This approach exploits plasticity in two different ways: On the one hand, due to plasticity desynchronizing stimulation may decrease the strength of the neurons' synapses by decreasing the rate of coincidences. On the other hand, neuronal networks with synaptic plasticity may exhibit bi- or multistability (Seliger et al. 2002; Tass and Majtanik 2006; Hauptmann and Tass 2007; Tass and Hauptmann 2007; Maistrenko et al. 2007). Accordingly, by decreasing the mean synaptic weight, desynchronizing stimulation may shift a neuronal population from a stable synchronized (pathological) state to a stable desynchronized (healthy) state, where the neuronal population remains thereafter, if left unperturbed. In Fig. 13 an exemplary simulation of a model neural network is displayed, for further details concerning the mathematical model we refer to references (Hauptmann and Tass 2007; Tass and Hauptmann 2007). Induced by appropriate stimulation protocols a switching between the different stable states is realizable. Starting from a desynchronized state, associated with a physiological model dynamics, low-frequency

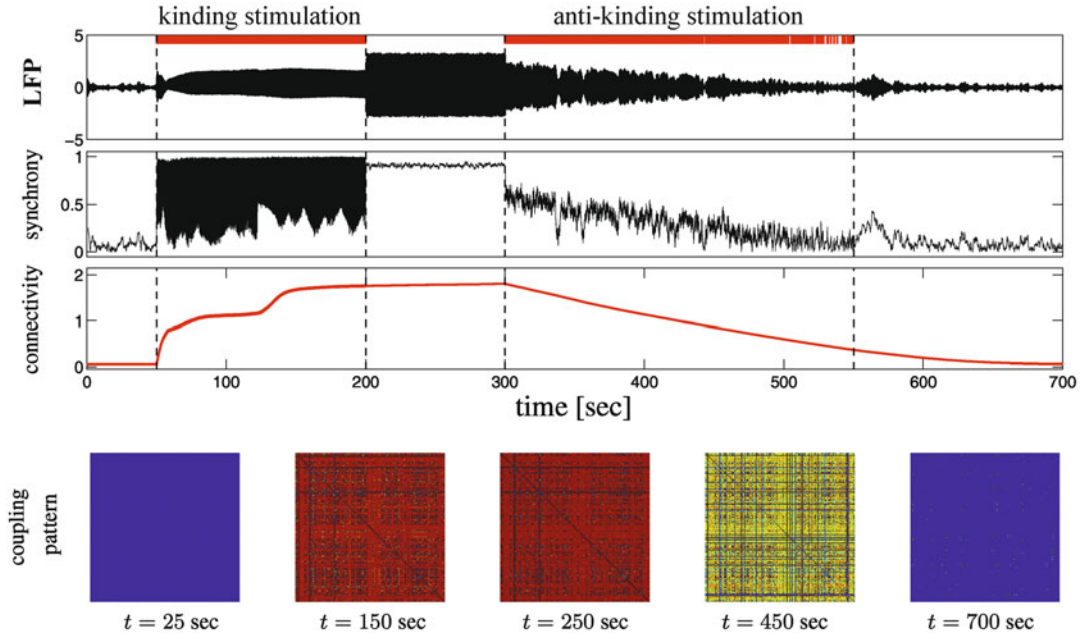

Brain Pacemaker, Fig. 13 Effects of kindling and anti-kindling stimulation on a population of model neurons. Low frequency stimulation is applied between 50 and 200 s, and CR stimulation (see section "Coordinated Reset Stimulation") is applied between 300 and 550 s. The local field potential, the level of synchronization within the network and the mean connectivity is plotted (from top to bottom). Five patterns representing the coupling topology of the network at different times are plotted below. *Blue* (*red*) colors represent low (high) values of the interneuronal connectivity

stimulation can induce a kindling of the synaptic connectivity and causes a stabilization of the synchronized state. After stimulation offset, the system remains in the pathological state (Fig. 13). In contrast, desynchronizing CR stimulation (see section "Coordinated Reset Stimulation") results in an anti-kindling of the pathological connectivity and, finally, the physiological weakly coupled and desynchronized state is reestablished (Fig. 13).

From a mathematical point of view, in a first approximation this situation may be illustrated by considering a double well potential, where each minimum corresponds to a stable attractor, surrounded by a basin of attraction (Fig. 14). The strongly synchronized state (*Pathol.* in Fig. 14) serves as a model for a disease state, whereas the uncorrelated or weakly synchronized state (*Healthy* in Fig. 14) is used as a model for a healthy state. As soon as the system, i.e., the neuronal population (illustrated by the *ball* in Fig. 14), enters a particular basin of attraction, it gets attracted by the corresponding attractor, so that it relaxes towards the corresponding minimum of the potential.

Appropriate stimulation protocols may shift the neuronal population from one state to another. Kindling stimulation of appropriate duration shifts the neuronal population from a desynchronized state close to a strongly synchronized state or at least into the basin of attraction of such a state (Fig. 14a, *red trajectory* from *Healthy* to *Pathol.*). Conversely, anti-kindling can be achieved by means of a desynchronizing stimulation which shifts the neuronal population close to the desynchronized state (Tass and Majtanik 2006; Hauptmann and Tass 2007, 2009, 2010; Tass and Hauptmann 2007; Tass and Popovych 2012; Popovych and Tass 2012) (Fig. 14b, *red trajectory* from *Pathol.* to *Healthy*). However, with respect to the long-term anti-kindling outcome, it is even sufficient to move the neuronal population from the synchronized state just into the basin of attraction of the desynchronized state (Fig. 14c, *red trajectory* from *Pathol.* to the intermediate state). After stimulus offset there may still be pronounced synchrony, but being captured within the basin of attraction of the desynchronized state, without further intervention the neuronal population spontaneously relaxes to the desynchronized state (Fig. 14c, *blue trajectory* from the intermediate state to *Healthy*). Note the short as well as the long desynchronizing stimulation in this schematic illustration have the same long-term anti-kindling outcome.

In PD neuronal populations of the basal ganglia are strongly synchronized (Beurrier et al. 2002; Schnitzler et al. 2006; Timmermann et al. 2007) and synaptic plasticity results in a further

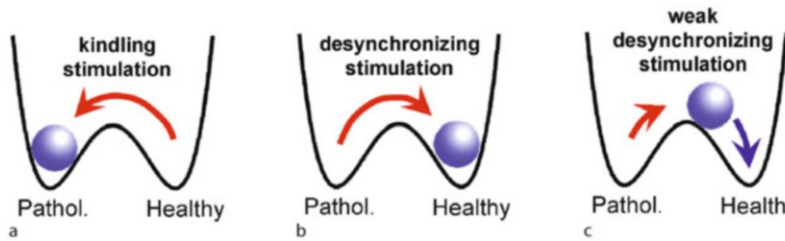

Brain Pacemaker, Fig. 14 Kindling and anti-kindling stimulation can move the neuronal population from one attractor to another: Schematic plot of the attractors symbolizing pathological (*Pathol.*) or healthy (*Healthy*) dynamical model states. (**a**) Periodic, kindling stimulation (*red trajectory*) shifts the population from a healthy, desynchronized state (*Healthy*) to a pathological, synchronized state (*Pathol.*). (**b**) Conversely, desynchronizing stimulation shifts the population from a pathological state (*Pathol.*) to the healthy uncorrelated state (*Healthy*). This anti-kindling is achieved by a desynchronizing stimulation of sufficient duration, so that after stimulus offset the population is close to the healthy state (*red trajectory*). (**c**) Alternatively, the same long-term anti-kindling effect can be achieved with a brief desynchronizing stimulation, which shifts the population to an intermediate state (*red trajectory*), which may still be connected with pronounced synchrony. However, since the intermediate state (*blue ball*) lies within the basin of attraction of a healthy state (*Healthy*) the population spontaneously relaxes to the healthy state without any further intervention (*blue trajectory*)

amplification of the synchronized activity by a strengthening of the synaptic connections (Nowotny et al. 2003). Properly designed electrical stimulation may be used to break this vicious circle and to induce an anti-kindling (Tass and Majtanik 2006; Hauptmann and Tass 2007, 2009, 2010; Tass and Hauptmann 2007; Tass and Popovych 2012; Popovych and Tass 2012), which finally might reestablish the normal level of connectivity, associated with a mostly uncorrelated neuronal activity. In this way a sustained long-lasting desynchronization can be achieved, and therapeutic after-effects can be expected after the cessation of desynchronizing stimulation as predicted computationally (see references above). In parkinsonian MPTP monkeys it was shown that unilateral CR stimulation delivered to the subthalamic nucleus (STN) for only 2 h per day during 5 days leads to significant and sustained therapeutic aftereffects for at least 30 days, while standard 130 Hz DBS has no aftereffects (Tass et al. 2012b).

Closed-Loop DBS

The standard setup of HF DBS assumes an open-loop stimulation protocol, where, after the corresponding parameter calibration, a permanent HF electrical pulse train is administered to the target nucleus without relation to the ongoing neuronal activity (Benabid et al. 1991; Volkmann 2004). Both, clinical studies and modeling studies systematically investigated the influence of stimulation parameters and focused on the optimization of the standard HF DBS via an appropriate parameter calibration (Rizzone et al. 2001; Moro et al. 2002; Rubin and Terman 2004) including a closed-loop optimization setup (Feng et al. 2007a, b).

In monkeys rendered parkinsonian with the neurotoxin MPTP a closed-loop DBS has been tested under acute conditions (Rosin et al. 2011). To this end, a short train (comprising seven pulses at 130 Hz) was delivered through a pair of electrodes located in the GPi at a predetermined, fixed latency (80 ms) following each action potential recorded through an electrode placed in the primary motor cortex (M1). This type of stimulation caused a strong decrease of the firing rate of the pallidal neurons together with a pronounced decrease of the oscillatory neuronal activity at tremor frequency (4–7 Hz) and at double tremor frequency (9–15 Hz) along with an amelioration of the MPTP-induced akinesia. After cessation of this type of closed-loop DBS the initial firing pattern reverted back, i.e., pallidal firing rate and pallidal oscillatory activity attained pre-stimulus levels (Rosin et al. 2011). In contrast, standard continuous 130 Hz DBS caused a less pronounced decrease of the pallidal firing rate, the oscillatory neuronal activity and the amelioration of the akinesia (Rosin et al. 2011).

Another study (Little et al. 2013) confirmed the efficacy of the closed-loop adaptive DBS (aDBS) in PD patients, where the onsets and offsets of HF stimulation were triggered by a threshold crossing by LFP in beta band measured via the same stimulation electrode implanted in STN. The stimulation trigger threshold for the LFP amplitude was heuristically determined in such a way that a reduction of the stimulation time of approximately 50% was achieved while maintaining clinical effect. The onset of HF stimulation was delayed by 30–40 ms after the crossing of the threshold by LFP, and the stimulation was sustained until beta amplitude fell below the threshold again (Little et al. 2013). For the same stimulation intensity and stimulation frequency (130 Hz), the aDBS can be about 30% more effective than standard continuous HF DBS, while less than 50% of the total electrical energy is delivered in the aDBS mode as compared to continuous HF DBS. Moreover, despite of the used fixed beta threshold, the triggered stimulation duration (per 10-s block) progressively drops over time during stimulation in the aDBS mode, which suggests that aDBS may lead to positive adaptive effects in pathological Parkinsonian networks (Little et al. 2013).

Summary

High-frequency deep brain stimulation is the golden standard for the treatment of medically refractory movement disorders (Benabid et al. 1991; Volkmann 2004).

Apart from the empirically developed standard DBS protocols (Benabid et al. 1991; Volkmann 2004), new stimulation approaches were successfully tested in pre-clinical and early clinical settings. For instance, a closed-loop neurostimulation controlled by beta-band activity showed a better performance than classical DBS in reducing motor signs as well as pallidal firing rate and oscillatory activity in parkinsonian nonhuman primates and PD patients (Rosin et al. 2011; Little et al. 2013).

Another approach, i.e., the model-based development of novel deep brain stimulation techniques, especially targets the pathological neuronal synchrony associated with Parkinson's disease (Tass 1999). This approach bases on dynamic neuronal self-organization principles and fundamental plasticity rules of the nervous system (Fig. 15) (Tass and Majtanik 2006; Tass and Hauptmann 2006, 2007; Hauptmann and Tass 2007, 2009, 2010; Tass and Popovych 2012; Popovych and Tass 2012).

The control methods discussed in this article differ to each other with respect to the stimulation setup and stimulation effects as well as other properties such as robustness and applicability. For example, CR stimulation in an open-loop protocol uses standard stimulation pulses (as used for HF stimulation) applied in a dedicated pattern and its technical realization was proven to be feasible (Hauptmann et al. 2009; Tass et al. 2012b). CR does not require sophisticated calibration and effectively causes transient desynchronization of the stimulated oscillators via a stimulation-induced cluster state. As mentioned in section "Coordinated Reset Stimulation," a number of computational, experimental and pre-clinical studies confirmed the applicability and efficacy of CR stimulation under different stimulation modalities.

Other smart feedback methods are more difficult to realize conceptually and technically and await experimental proof of concept, see sections "Multisite Linear Delayed Feedback," "Nonlinear Delayed

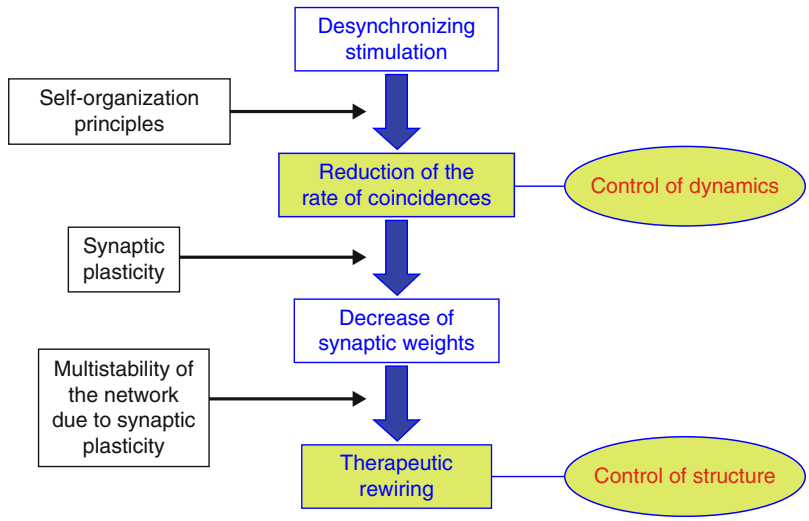

Brain Pacemaker, Fig. 15 Schematic illustration of unlearning of pathological connectivity by desynchronizing stimulation. The latter reduces the overall rate of coincidences in the neuronal population. This is effectively achieved by using dynamic self-organization principles. The reduction of the rate of coincidences, in turn, reduces the synaptic weights and shifts the stimulated network in a weakly coupled state. Because of the multistability, not only strongly coupled and synchronized states, but also weakly coupled and weakly synchronized states are stable. Accordingly, the neuronal population stably remains in a desynchronized or weakly synchronized state, after having been shifted into the basin of attraction of that state by means of desynchronizing stimulation. Hence, a suitable control of the dynamics of the network can lead to long-lasting changes of its connectivity and dynamics (First published in Tass and Hauptmann (2007). Used with permission from the *International Journal of Psychophysiology*)

Feedback," and "Proportional–Integro–Differential Feedback." In modeling studies they effectively result in a sustained desynchronized regime. The feedback methods can be applied under a variety of conditions, and possess an intrinsic demand-controlled character, where the stimulation signal is significantly reduced or even vanishes as soon as desynchronization is achieved. The experimental and clinical realization of these methods is a challenging task, first of all, from the technical side, since stimulation signals have to fulfill all safety aspects like charge density limits. These limits strongly affect the applicability of the slow feedback signals, i.e., slow compared to the timescales of HF and CR pulses. In this way, the application conditions of the methods have to be handled with care, and stimulation setups and effects have to clearly be distinguished for different feedback methods. Otherwise, one can come up with misleading conclusions and erroneous interpretations of the efficacy of feedback methods, see the computational study (Dovzhenok et al. 2013) where nonlinear and linear techniques were not properly distinguished. To this end, only an experimental proof of concept can finally assess the applicability and performance of the control methods.

In forthcoming studies the mathematical modeling needs to be refined to incorporate further anatomical and physiological details, for instance, the contributions of glial cells (Silchenko and Tass 2008). By the same token, control techniques have to be optimized and further developed. As currently done for CR stimulation (Tass et al. 2012b), clinical studies are necessary to evaluate the therapeutic effects of the novel stimulation techniques under real conditions. This interdisciplinary endeavor might finally provide superior therapies for patients with neurological or psychiatric diseases.

Bibliography

Abbott L, Nelson S (2000) Synaptic plasticity: taming the beast. Nat Neurosci 3:1178–1183

Adamchic I, Toth T, Hauptmann C, Tass PA (2013) Reversing pathologically increased electroencephalogram power by acoustic coordinated reset neuromodulation. Hum Brain Mapp 35(5):2099–2118

Alberts WW, Wright EJ, Feinstein B (1969) Cortical potentials and parkinsonian tremor. Nature 221:670–672

Anderson ME, Postupna N, Ruffo M (2003) Effects of high-frequency stimulation in the internal globus pallidus on the activity of thalamic neurons in the awake monkey. J Neurophysiol 89(2):1150–1160

Andres F, Gerloff C (1999) Coherence of sequential movements and motor learning. J Clin Neurophysiol 16(6):520–527

Benabid A, Pollak P, Louveau A, Henry S, de Rougemont JJ (1987) Combined (thalamotomy and stimulation) stereotactic surgery of the VIM thalamic nucleus for bilateral Parkinson disease. Appl Neurophysiol 50(1-6):344–346

Benabid AL, Pollak P, Gervason C, Hoffmann D, Gao DM, Hommel M, Perret JE, de Rougemount J (1991) Long-term suppression of tremor by chronic stimulation of ventral intermediate thalamic nucleus. Lancet 337:403–406

Benabid AL, Benazzous A, Pollak P (2002) Mechanisms of deep brain stimulation. Mov Disord 17:73–74

Benabid A-L, Wallace B, Mitrofanis J, Xia R, Piallat B, Chabardes S, Berger F (2005) A putative gerneralized model of the effects and mechanism of action of high frequency electrical stimulation of the central nervous system. Acta Neurol Belg 105:149–157

Beurrier C, Bioulac B, Audin J, Hammond C (2001) High-frequency stimulation produces a transient blockade of voltage-gated currents in subthalamic neurons. J Neurophysiol 85(4):1351–1356

Beurrier C, Garcia L, Bioulac B, Hammond C (2002) Subthalamic nucleus: a clock inside basal ganglia? Thalamus Relat Syst 2:1–8

Blond S, Caparros-Lefebvre D, Parker F, Assaker R, Petit H, Guieu J-D, Christiaens J-L (1992) Control of tremor and involuntary movement disorders by chronic stereotactic stimulation of the ventral intermediate thalamic nucleus. J Neurosurg 77:62–68

Brice J, McLellan L (1980) Suppression of intention tremor by contingent deep-brain stimulation. Lancet 1(8180):1221–1222

Daido H (1992) Order function and macroscopic mutual entrainment in uniformly coupled limit-cycle oscillators. Prog Theor Phys 88:1213–1218

Danzl P, Hespanha J, Moehlis J (2009) Event-based minimum-time control of oscillatory neuron models. Biol Cybern 101(5–6):387–399

Debanne D, Gahweiler B, Thompson S (1998) Long-term synaptic plasticity between pairs of individual CA3 pyramidal cells in rat hippocampus slice cultures. J Physiol 507:237–247

Deuschl G, Schade-Brittinger C, Krack P, Volkmann J, Schäfer H, Bötzel K, Daniels C, Deutschländer A, Dillmann U, Eisner W, Gruber D, Hamel W, Herzog J, Hilker R, Klebe S, Kloß M, Koy J, Krause M, Kupsch A, Lorenz D, Lorenzl S, Mehdorn H, Moringlane J, Oertel W, Pinsker M, Reichmann H, Reuß A, Schneider G-H, Schnitzler A, Steude U, Sturm V, Timmermann L, Tronnier V,

Trottenberg T, Wojtecki L, Wolf E, Poewe W, Voges J (2006) A randomized trial of deep-brain stimulation for Parkinson's disease. N Engl J Med 355:896–908
Dolan K, Majtanik M, Tass P (2005) Phase resetting and transient desynchronization in networks of globally coupled phase oscillators with inertia. Physica D 211:128–138
Dovzhenok A, Park C, Worth RM, Rubchinsky LL (2013) Failure of delayed feedback deep brain stimulation for intermittent pathological synchronization in Parkinson's disease. PLoS One 8(3):e58264
Elble RJ, Koller WC (1990) Tremor. John Hopkins University Press, Baltimore
Ermentrout B, Kopell N (1991) Multiple pulse interactions and averaging in systems of coupled neural assemblies. J Math Biol 29:195–217
Feldman D (2000) Timing-based LTP and LTD at vertical inputs to layer II/III pyramidal cells in rat barrel cortex. Neuron 27:45–56
Feng X, Greenwald B, Rabitz H, Shea-Brown E, Kosut R (2007a) Toward closed-loop optimization of deep brain stimulation for Parkinson's disease: concepts and lessons from a computational model. J Neural Eng 4(2): L14–L21
Feng XJ, Shea-Brown E, Greenwald B, Kosut R, Rabitz H (2007b) Optimal deep brain stimulation of the subthalamic nucleus – a computational study. J Comput Neurosci 23(3):265–282
Filali M, Hutchison W, Palter V, Lozano A, Dostrovsky JO (2004) Stimulation-induced inhibition of neuronal firing in human subthalamic nucleus. Exp Brain Res 156:274–281
Freund H-J (2005) Long-term effects of deep brain stimulation in Parkinson's disease. Brain 128:2222–2223
Garcia L, D'Alessandro G, Fernagut P-O, Bioulac B, Hammond C (2005) Impact of high-frequency stimulation parameters on the pattern of discharge of subthalamic neurons. J Neurophysiol 94:3662–3669
Gerstner W, Kempter R, van Hemmen J, Wagner H (1996) A neuronal learning rule for sub-millisecond temporal coding. Nature 383:76–78
Gildenberg P (2005) Evolution of neuromodulation. Stereotact Funct Neurosurg 83:71–79
Goddar G (1967) Development of epileptic seizures through brain stimulation at low intensity. Nature 214:1020–1021
Gradinaru V, Mogri M, Thompson KR, Henderson JM, Deisseroth K (2009) Optical deconstruction of parkinsonian neural circuitry. Science 324(5925):354–359
Grannan ER, Kleinfeld D, Sompolinsky H (1993) Stimulus-dependent synchronization of neuronal assemblies. Neural Comput 5:550–569
Grill WM, McIntyre CC (2001) Extracellular excitation of central neurons: implications for the mechanisms of deep brain stimulation. Thalamus Relat Syst 1:269–277
Haken H (1970) Laser theory, vol XXV/2C. Encyclopedia of physics. Springer, Berlin
Haken H (1977) Synergetics. An introduction. Springer, Berlin
Haken H (1983) Advanced synergetics. Springer, Berlin
Haken H (1996) Principles of brain functioning. A synergetic approach to brain activity, behavior, cognition. Springer, Berlin
Haken H (2002) Brain dynamics. Synchronization and activity patterns in pulse-coupled neural nets with delays and noise. Springer, Berlin
Haken H, Kelso J, Bunz H (1985) A theoretical model of phase transitions in human hand movements. Biol Cybern 51:347–356
Hammond C, Ammari R, Bioulac B, Garcia L (2008) Latest view on the mechanism of action of deep brain stimulation. Mov Disord 23(15):2111–2121
Hansel D, Mato G, Meunier C (1993a) Phase dynamics of weakly coupled Hodgkin–Huxley neurons. Europhys Lett 23:367–372
Hansel D, Mato G, Meunier C (1993b) Phase reduction and neural modeling. Concepts Neurosci 4(2):193–210
Hashimoto T, Elder C, Okun M, Patrick S, Vitek J (2003) Stimulation of the subthalamic nucleus changes the firing pattern of pallidal neurons. J Neurosci 23(5):1916–1923
Hauptmann C, Tass PA (2007) Therapeutic rewiring by means of desynchronizing brain stimulation. Biosystems 89:173–181
Hauptmann C, Tass PA (2009) Cumulative and after-effects of short and weak coordinated reset stimulation: a modeling study. J Neural Eng 6(1):016004
Hauptmann C, Tass PA (2010) Restoration of segregated, physiological neuronal connectivity by desynchronizing stimulation. J Neural Eng 7:056008
Hauptmann C, Popovych O, Tass PA (2005a) Delayed feedback control of synchronization in locally coupled neuronal networks. Neurocomputing 65–66:759–767
Hauptmann C, Popovych O, Tass PA (2005b) Effectively desynchronizing deep brain stimulation based on a coordinated delayed feedback stimulation via several sites: a computational study. Biol Cybern 93:463–470
Hauptmann C, Popovych O, Tass PA (2005c) Multisite coordinated delayed feedback for an effective desynchronization of neuronal networks. Stochastics Dyn 5(2):307–319
Hauptmann C, Omelchenko O, Popovych OV, Maistrenko Y, Tass PA (2007a) Control of spatially patterned synchrony with multisite delayed feedback. Phys Rev E 76:066209
Hauptmann C, Popovych O, Tass P (2007b) Desynchronizing the abnormally synchronized neural activity in the subthalamic nucleus: a modeling study. Expert Rev Med Devices 4(5):633–650
Hauptmann C, Roulet JC, Niederhauser JJ, Doll W, Kirlangic ME, Lysyansky B, Krachkovskyi V, Bhatti MA, Barnikol UB, Sasse L, Buhrle CP, Speckmann EJ, Gotz M, Sturm V, Freund HJ, Schnell U, Tass PA (2009) External trial deep brain stimulation device for the application of desynchronizing stimulation techniques. J Neural Eng 6(6):066003
Hebb D (1949) The organization of behavior. Wiley, New York

Kelso J (1995) Dynamic patterns: the self-organization of brain and behavior. MIT Press, Cambridge, MA

Kilgard M, Merzenich M (1998) Cortical map reorganization enabled by nucleus basalis activity. Science 279:1714–1718

Kiss IZ, Rusin CG, Kori H, Hudson JL (2007) Engineering complex dynamical structures: sequential patterns and desynchronization. Science 316(5833):1886–1889

Kumar R, Lozano A, Sime E, Lang A (2003) Long-term follow-up of thalamic deep brain stimulation for essential and parkinsonian tremor. Neurology 61:1601–1604

Kuramoto Y (1984) Chemical oscillations, waves, turbulence. Springer, Berlin/Heidelberg/New York

Lenz F, Kwan H, Martin R, Tasker R, Dostrovsky J, Lenz Y (1994) Single unit analysis of the human ventral thalamic nuclear group. Tremor-related activity in functionally identified cells. Brain 117:531–543

Limousin P, Speelman J, Gielen F, Janssens M (1999) Multicentre European study of thalamic stimulation in parkinsonian and essential tremor. J Neurol Neurosurg Psychiatry 66(3):289–296

Little S, Pogosyan A, Neal S, Zavala B, Zrinzo L, Hariz M, Foltynie T, Limousin P, Ashkan K, FitzGerald J, Green AL, Aziz TZ, Brown P (2013) Adaptive deep brain stimulation in advanced Parkinson disease. Ann Neurol 74(3):449–457

Luecken L, Yanchuk S, Popovych OV, Tass PA (2013) Desynchronization boost by non-uniform coordinated reset stimulation in ensembles of pulse-coupled neurons. Front Comput Neurosci 7:63

Luo M, YJ W, Peng JH (2009) Washout filter aided mean field feedback desynchronization in an ensemble of globally coupled neural oscillators. Biol Cybern 101(3):241–246

Lysyansky B, Popovych OV, Tass PA (2011a) Desynchronizing anti-resonance effect of m: n on–off coordinated reset stimulation. J Neural Eng 8(3):036019

Lysyansky B, Popovych OV, Tass PA (2011b) Multifrequency activation of neuronal networks by coordinated reset stimulation. Interface Focus 1(1):75–85

Lysyansky B, Popovych OV, Tass PA (2013) Optimal number of stimulation contacts for coordinated reset neuromodulation. Front Neuroeng 6:5

Maistrenko Y, Lysyansky B, Hauptmann C, Burylko O, Tass P (2007) Multistability in the Kuramoto model with synaptic plasticity. Phys Rev E 75:066207

Majtanik M, Dolan K, Tass P (2006) Desynchronization in networks of globally coupled neurons with dendritic dynamics. J Biol Phys 32:307–333

Markram H, Lübke J, Frotscher M, Sakmann B (1997) Regulation of synaptic efficacy by coincidence of postsynaptic APs and EPSPs. Science 275:213–215

McIntyre C, Grill W, Sherman D, Thakor N (2004a) Cellular effects of deep brain stimulation: model-based analysis of activation and inhibition. J Neurophysiol 91:1457–1469

McIntyre CC, Savasta M, Goff KKL, Vitek J (2004b) Uncovering the mechanism(s) of action of deep brain stimulation: activation, inhibition, or both. Clin Neurophysiol 115:1239–1248

Meissner W, Leblois A, Hansel D, Bioulac B, Gross CE, Benazzouz A, Boraud T (2005) Subthalamic high frequency stimulation resets subthalamic firing and reduces abnormal oscillations. Brain 128:2372–2382

Milton J, Jung P (eds) (2003) Epilepsy as a dynamics disease. Springer, Berlin

Miocinovic S, Parent M, Butson C, Hahn P, Russo G, Vitek J, McIntyre C (2006) Computational analysis of subthalamic nucleus and lenticular fasciculus activation during therapeutic deep brain stimulation. J Neurophysiol 96:1569–1580

Morimoto K, Fahnestock M, Racine R (2004) Kindling and status epilepticus models of epilepsy: rewiring the brain. Prog Neurobiol 73:1–60

Moro E, Esselink RJA, Xie J, Hommel M, Benabid AL, Pollak P (2002) The impact on Parkinson's disease of electrical parameter settings in STN stimulation. Neurology 59(5):706–713

Nabi A, Moehlis J (2011) Single input optimal control for globally coupled neuron networks. J Neural Eng 8(6):065008

Neiman A, Russell D, Yakusheva T, DiLullo A, Tass PA (2007) Response clustering in transient stochastic synchronization and desynchronization of coupled neuronal bursters. Phys Rev E 76:021908

Nini A, Feingold A, Slovin H, Bergmann H (1995) Neurons in the globus pallidus do not show correlated activity in the normal monkey, but phase-locked oscillations appear in the MPTP model of parkinsonism. J Neurophysiol 74:1800–1805

Nowotny T, Zhigulin V, Selverston A, Abarbanel H, Rabinovich M (2003) Enhancement of synchronization in a hybrid neural circuit by spike-timing dependent plasticity. J Neurosci 23:9776–9785

Pikovsky A, Rosenblum M, Kurths J (2001) Synchronization, a universal concept in nonlinear sciences. Cambridge University Press, Cambridge

Pliss V (1964) Principal reduction in the theory of stability of motion. Izv Akad Nauk SSSR Math Ser 28:1297–1324

Popovych OV, Tass PA (2010) Synchronization control of interacting oscillatory ensembles by mixed nonlinear delayed feedback. Phys Rev E 82(2):026204

Popovych OV, Tass PA (2012) Desynchronizing electrical and sensory coordinated reset neuromodulation. Front Hum Neurosci 6:58

Popovych OV, Hauptmann C, Tass PA (2005) Effective desynchronization by nonlinear delayed feedback. Phys Rev Lett 94:164102

Popovych OV, Hauptmann C, Tass PA (2006a) Control of neuronal synchrony by nonlinear delayed feedback. Biol Cybern 95:69–85

Popovych OV, Hauptmann C, Tass PA (2006b) Desynchronization and decoupling of interacting oscillators by nonlinear delayed feedback. Int J Bif Chaos 16(7):1977–1987

Pyragas K, Popovych OV, Tass PA (2007) Controlling synchrony in oscillatory networks with a separate stimulation-registration setup. Europhys Lett 80:40002

Pyragas K, Novicenko V, Tass P (2013) Mechanism of suppression of sustained neuronal spiking under high-frequency stimulation. Biol Cybern 107(6):669–684

Rizzone M, Lanotte M, Bergamasco B, Tavella A, Torre E, Faccani G, Melcarne A, Lopiano L (2001) Deep brain stimulation of the subthalamic nucleus in Parkinson's disease: effects of variation in stimulation parameters. J Neurol Neurosurg Psychiatry 71(2):215–219

Rodriguez-Oroz M, Obeso J, Lang A, Houeto J, Pollak P, Rehncrona S, Kulisevsky J, Albanese A, Volkmann J, Hariz M, Quinn N, Speelman J, Guridi J, Zamarbide I, Gironell A, Molet J, Pascual-Sedano B, Pidoux B, Bonnet A, Agid Y, Xie J, Benabid A, Lozano A, Saint-Cyr J, Romito L, Contarino M, Scerrati M, Fraix V, Blercom NV (2005) Bilateral deep brain stimulation in Parkinson's disease: a multicentre study with 4 years follow-up. Brain 128:2240–2249

Rosenblum MG, Pikovsky AS (2004a) Controlling synchronization in an ensemble of globally coupled oscillators. Phys Rev Lett 92:114102

Rosenblum MG, Pikovsky AS (2004b) Delayed feedback control of collective synchrony: an approach to suppression of pathological brain rhythms. Phys Rev E 70:041904

Rosin B, Slovik M, Mitelman R, Rivlin-Etzion M, Haber SN, Israel Z, Vaadia E, Bergman H (2011) Closed-loop deep brain stimulation is superior in ameliorating parkinsonism. Neuron 72(2):370–384

Rubin JE, Terman D (2004) High frequency stimulation of the subthalamic nucleus eliminates pathological thalamic rhythmicity in a computational model. J Comput Neurosci 16(3):211–235

Schnitzler A, Timmermann L, Gross J (2006) Physiological and pathological oscillatory networks in the human motor system. J Physiol Paris 99(1):3–7

Schöner G, Haken H, Kelso J (1986) A stochastic theory of phase transitions in human hand movement. Biol Cybern 53:247–257

Schuurman PR, Bosch DA, Bossuyt PM, Bonsel GJ, van Someren EJ, de Bie RM, Merkus MP, Speelman JD (2000) A comparison of continuous thalamic stimulation and thalamotomy for suppression of severe tremor. N Engl J Med 342:461–468

Seliger P, Young S, Tsimring L (2002) Plasticity and learning in a network of coupled phase oscillators. Phys Rev E 65:041906

Shen K, Zhu Z, Munhall A, Johnson SW (2003) Synaptic plasticity in rat subthalamic nucleus induced by high-frequency stimulation. Synapse 50:314–319

Silchenko A, Tass P (2008) Computational modeling of paroxysmal depolarization shifts in neurons induced by the glutamate release from astrocytes. Biol Cybern 98:61–74

Silchenko AN, Adamchic I, Hauptmann C, Tass PA (2013) Impact of acoustic coordinated reset neuromodulation on effective connectivity in a neural network of phantom sound. NeuroImage 77:133–147

Singer W (1989) Search for coherence: a basic principle of cortical self-organization. Concepts Neurosci 1:1–26

Smirnov DA, Barnikol UB, Barnikol TT, Bezruchko BP, Hauptmann C, Buhrle C, Maarouf M, Sturm V, Freund H-J, Tass PA (2008) The generation of parkinsonian tremor as revealed by directional coupling analysis. Europhys Lett 83(2):20003

Song S, Miller K, Abbott L (2000) Competitive Hebbian learning through spike-timing-dependent synaptic plasticity. Nat Neurosci 3(9):919–926

Speckmann E, Elger C (1991) The neurophysiological basis of epileptic activity: a condensed overview. Epilepsy Res Suppl 2:1–7

Steriade M, Jones EG, Llinas RR (1990) Thalamic oscillations and signaling. Wiley, New York

Strogatz SH (2003) Sync: the emerging science of spontaneous order. Hyperion Books, New York

Tasker RR (1998) Deep brain stimulation is preferable to thalamotomy for tremor suppression. Surg Neurol 49:145–154

Tass PA (1996a) Phase resetting associated with changes of burst shape. J Biol Phys 22:125–155

Tass PA (1996b) Resetting biological oscillators – a stochastic approach. J Biol Phys 22:27–64

Tass PA (1999) Phase resetting in medicine and biology: stochastic modelling and data analysis. Springer, Berlin

Tass PA (2000) Stochastic phase resetting: a theory for deep brain stimulation. Prog Theor Phys Suppl 139:301–313

Tass PA (2001a) Desynchronizing double-pulse phase resetting and application to deep brain stimulation. Biol Cybern 85:343–354

Tass PA (2001b) Effective desynchronization by means of double-pulse phase resetting. Europhys Lett 53:15–21

Tass PA (2001c) Effective desynchronization with a resetting pulse train followed by a single pulse. Europhys Lett 55:171–177

Tass PA (2002a) Desynchronization of brain rhythms with soft phase-resetting techniques. Biol Cybern 87:102–115

Tass PA (2002b) Effective desynchronization with a stimulation technique based on soft phase resetting. Europhys Lett 57:164–170

Tass PA (2002c) Effective desynchronization with bipolar double-pulse stimulation. Phys Rev E 66:036226

Tass PA (2003a) Desynchronization by means of a coordinated reset of neural sub-populations – a novel technique for demand-controlled deep brain stimulation. Prog Theor Phys Suppl 150:281–296

Tass PA (2003b) A model of desynchronizing deep brain stimulation with a demand-controlled coordinated reset of neural subpopulations. Biol Cybern 89:81–88

Tass PA, Hauptmann C (2006) Therapeutic rewiring by means of desynchronizing brain stimulation. Nonlinear Phenom Complex Syst 9(3):298–312

Tass P, Hauptmann C (2007) Therapeutic modulation of synaptic connectivity with desynchronizing brain stimulation. Int J Psychophysiol 64:53–61

Tass PA, Majtanik M (2006) Long-term anti-kindling effects of desynchronizing brain stimulation: a theoretical study. Biol Cybern 94:58–66

Tass PA, Popovych OV (2012) Unlearning tinnitus-related cerebral synchrony with acoustic coordinated reset stimulation: theoretical concept and modelling. Biol Cybern 106:27–36

Tass PA, Hauptmann C, Popovych OV (2006) Development of therapeutic brain stimulation techniques with methods from nonlinear dynamics and statistical physics. Int J Bif Chaos 16(7):1889–1911

Tass PA, Silchenko AN, Hauptmann C, Barnikol UB, Speckmann EJ (2009) Long-lasting desynchronization in rat hippocampal slice induced by coordinated reset stimulation. Phys Rev E 80(1):011902

Tass P, Adamchic I, Freund H-J, von Stackelberg T, Hauptmann C (2012a) Counteracting tinnitus by acoustic coordinated reset neuromodulation. Restor Neurol Neurosci 30:367–374

Tass PA, Qin L, Hauptmann C, Doveros S, Bezard E, Boraud T, Meissner WG (2012b) Coordinated reset has sustained aftereffects in parkinsonian monkeys. Ann Neurol 72:816–820

Timmermann L, Florin E, Reck C (2007) Pathological cerebral oscillatory activity in Parkinson's disease: a critical review on methods, data and hypotheses. Expert Rev Med Devices 4(5):651–661

Tukhlina N, Rosenblum M, Pikovsky A, Kurths J (2007) Feedback suppression of neural synchrony by vanishing stimulation. Phys Rev E 75:011918

van Hemmen J (2001) Theory of synaptic plasticity. In: Moss F, Gielen S (eds) Handbook of biological physics, vol 4. Elsevier, Amsterdam, pp 771–823

Volkmann J (2004) Deep brain stimulation for the treatment of Parkinson's disease. J Clin Neurophysiol 21:6–17

Welter ML, Houeto JL, Bonnet AM, Bejjani PB, Mesnage V, Dormont D, Navarro S, Cornu P, Agid Y, Pidoux B (2004) Effects of high-frequency stimulation on subthalamic neuronal activity in parkinsonian patients. Arch Neurol 61(1):89–96

Winfree A (1980) The geometry of biological time. Springer, Berlin

Wunderlin A, Haken H (1975) Scaling theory for non-equilibrium systems. Z Phys B 21:393–401

Zhai Y, Kiss IZ, Tass PA, Hudson JL (2005) Desynchronization of coupled electrochemical oscillators with pulse stimulations. Phys Rev E 71:065202

Zhai Y, Kiss IZ, Hudson JL (2008) Control of complex dynamics with time-delayed feedback in populations of chemical oscillators: desynchronization and clustering. Ind Eng Chem Res 47(10):3502–3514

Zhou Q, Tao H, Poo M (2003) Reversal and stabilization of synaptic modifications in a developing visual system. Science 300:1953–1957